



UNIVERSITAT DE
BARCELONA

Comparative life cycle assessment (LCA): Conventional TES system versus alternative steel slag-based TES system for CSP plants.

Author: Carlos A. Vielma Leal

Tutors: Dr. Alejandro Calderón Díaz

Dr. Adela Svobodova

Academic course: 2022 - 2023

Master in Renewable Energy and
Energy Sustainability

Dos Campus d'Excel·lència Internacional:



Contents

1	Introduction.....	1
2	General objective.....	3
2.1	Specific objectives	3
3	Materials and methods.....	3
3.1	Description of the considered CSP Plant	3
3.2	Description of the TES system considered.....	5
3.2.1	EAF steel slag as thermal storage material.....	6
4	LCA Methodology	8
4.1	Life cycle assessment.....	8
4.1.1	LCA Goal and scope.....	10
4.1.2	Functional unit	10
4.1.3	System boundary.....	11
4.1.4	EAF steel slag perimeter: methodology to assign the impacts points	12
4.1.5	Sources of environmental and economic data	17
4.1.6	Impact inventory	18
4.1.7	Data inventory	18
5	Results and discussion	20
5.1	Life cycle inventory analysis	20
5.2	Life cycle impact assessment	22
5.2.1	By-product impacts estimation.....	22
5.2.2	TES and HTF system impact estimation.....	24
5.2.3	Global impact of the CSP Plant	26
5.3	Interpretation phase with a sustainability approach.....	28
6	Conclusion.....	30
7	References	31
8	Annexes	35
8.1	Annex I: Calculation of materials required in the TES and HTF system inventory for thermocline configuration.....	35
8.2	Annex II: Plots of processes and flows for the considered CSP Plants	38
8.3	Annex III: ReCiPe 2016 v1.1 (E/A) Complete impact categories data	41
	Abstract	49
	Resumen	50

List of Figures

Figure 1. CSP tower with thermocline TES system..	4
Figure 2. Thermocline tank working principle.	5
Figure 3. CSP Plant configurations: (a) Two-tanks TES system. (b) Thermocline TES System.....	6
Figure 4. Pictures of raw EAF slags samples showing their general appearance.....	7
Figure 5. The relationship among the four phases in an LCA.....	9
Figure 6. Impact categories that are covered in the ReCiPe2016 methodology.	10
Figure 7. System boundary of a concentrating solar power (CSP) plant.....	11
Figure 8. Theoretical multifunction process consisting of two separate sub-processes.	12
Figure 9. Description of the sub-systems involved in the study..	14
Figure 10. System boundaries of EAF steel slag-based packed bed filler.	15
Figure 11. Classification of the processing of manufacturing inventory data..	19
Figure 12. Materials demand associated to the TES and HTF Systems.....	22
Figure 13. Impacts' comparison of the two TESM used in the thermocline configuration.	24
Figure 14. Comparison of the impacts from each TES and HTF component.....	25
Figure 15. Global impact assessment of the CSP Plant.....	27
Figure 16. Comparative contribution of each TES and HTF System in the CSP plant.	27
Figure 17. Plots of processes and flows used in the CSP Plant with a conventional TES and HTF System.....	38
Figure 18. Plots of processes and flows used in the CSP Plant with a thermocline TES and HTF System.....	39
Figure 19. TES and HTF systems plots for each CSP Plant configuration.	40

List of Tables

Table 1. Characteristics of the assessed CSP tower plant..	4
Table 2. Physical properties of selected heat storage materials.....	7
Table 3. Physical properties and price of slag pebbles, taconite, and quartzite rock. ..	18
Table 4. Materials and consumptions inventory for the two CSP Plants.....	19
Table 5. By-product impact calculation: First scenario.	23
Table 6. By-product impact calculation: Second scenario.	23
Table 7. Environmental impacts associated to the TES and HTF System.....	25
Table 8. Global environmental impacts associated to the CSP Plant.	26
Table 9. Total impact IPCC method: GW20 indicator per kWh of net produced electricity.	28
Table 10. Scaling the Thermocline TES and HTF system inventory from the conventional plant inventory	37
Table 11. By-product complete impact categories data: First scenario.....	41
Table 12. By-product complete impact categories data: Second scenario.....	42
Table 13. Complete impact categories data: Conventional TES and HTF System	43
Table 14. Complete impact categories data: Thermocline TES and HTF System, First scenario.....	44
Table 15. Complete impact categories data: Thermocline TES and HTF System, Second scenario.....	46
Table 16. Complete impact categories data: Global environmental impacts associated to the CSP Plant.....	47

Glossary

TES	Thermal Energy Storage
CSP	Concentrating Solar Power
PCM	Phase Change Material
LCA	Life Cycle Assessment
IEA	International Energy Agency
EAF	Electric Arc Furnace
LCI	Life Cycle Inventory Analysis
LCIA	Life Cycle Impact Assessment
GWP	Global Warming Potential
ISO	International Organization for Standardization
RoW	Rest of the World
HTF	Heat Transfer Fluid
VSF	Volumetric Scale Factor
TESM	Thermal Energy Storage Material

1 Introduction

Thermal energy storage (TES) plays a crucial role in the journey towards decarbonization. Its integration into concentrating solar power (CSP) plants aims to enhance their performance and flexibility, enabling more efficient utilization of energy according to demand. CSP technology harnesses solar energy to generate heat, which can then be used to generate either electricity through a thermodynamic cycle (such as a Rankine, air-Brayton, etc), or direct thermal energy for process heat [1].

The advantage of CSP over other solar energy technology is having a thermal energy storage (TES) system. The TES refers to the process of storing thermal energy in a material or medium for later use (during night hours or when the sun power is insufficient). This enables sites to access dispatchable power by a three-step process: charging, storing, and discharging. However, current storage capacity in most CPS plants is considered low, generally sitting at about 7,5 h [2]. Although it may be generally not enough to provide power throughout all night, the development of this storage technology is opening the doors for further investigation to find alternatives materials that could work at higher operating temperatures leading to an improvement in the efficiency of the heat conversion to power.

From the most known three types of CSP plants – Parabolic trough, Heliostat power tower and Linear Fresnel reflector – the power towers have the best efficiency of electricity generation due to the temperatures achieved (the highest of them) and the transportation methods for the heat collected (lower heat is lost throughout the system because of using fewer piping) [3]. Based on this comparison, it can be expected that as technology continues to develop, heliostat power towers are likely to become the dominant CSP method and being a vehicle towards reaching decarbonisation by using TES systems.

Thermal energy storage systems come in two main configurations. The first is the two-tank configuration, with separate tanks for hot and cold molten salts. The second and more innovative is the thermocline configuration, using a single tank with a mixture of materials to create a temperature gradient, and simplifying the system. The Heat Transfer Fluid (HTF) is a crucial element in both types of configurations since it absorbs the solar energy and transfers it to the storage tanks. [4]

The most used TES systems (solid media, molten salts and PCM system) present different dimensions, storage capacity and final purposes. Oró et al. [3] 2012 compare these systems global impact (manufacturing + operational impact) in different scenarios and concluded that the molten salts present the highest global impact. Other Important disadvantages related to the use of molten salts in TES systems are notable, like the potential corrosion problems, the relatively high freezing point of most solar salts, and the fact that their higher outlet temperature means heat losses from the solar heat, requiring more expensive piping and materials [4].

Nevertheless, a key issue in the design of a thermal energy storage system is its thermal capacity [4], which continues to make molten salts configuration an interesting target to improve since this TES system can reach more than 500 °C.

This makes evident the necessity to evaluate new alternatives materials compatible with molten salts to transcend gradually from liquid TES systems to solid ones (easier to control) that can reach higher temperatures, increasing storage capacity and mechanical/chemical stability of the systems. Therefore, this materials replacement could contribute to have better efficiencies in a thermodynamic cycle and - consequentially - higher conversion to power.

According to the International Energy Agency (IEA), it is projected that CSP will account for approximately 9% of global electricity production by 2050. To achieve this target, the CSP industry would require over 10 million tons per year of thermal storage materials solely for this market [5]. No material currently meets the criteria of availability, technical performance, cost, and life cycle assessment. The EAF (Electric Arc Furnace) steel slag, main waste of the steel manufacturing industry, appears to be a promising candidate.

The utilization of steel slag for thermal energy storage (TES) applications has the potential to reduce waste and minimize environmental impact. International Energy Agency's target of 630 GWe of CSP by 2050 is equivalent to construct approximately 400 plants the size of Andasol (28.500 tons of Solar Salt) on an annual basis. Considering only the thermal properties of materials, this would result in a demand for approximately $19,8 \times 10^6$ tons of slag each year [6]. Furthermore, the incorporation of slag can extend the operating temperature of TES systems up to 1.000 °C (in certain conditions), while simultaneously reducing the system cost.

Nowadays, optimizing the TES system is practically mandatory, especially, since an increase in its size entails an increase in the size of several CSP components, such as the tower and the receiver. This naturally affect both the environmental impacts and the economic evaluation associated with the plant [7]. Therefore, the aim of this research is to perform a comparative Life Cycle Assessment (LCA) of an active direct TES system in a CSP plant by using EAF steel slag as a thermal storage material in a thermocline configuration with solar salt as heat transfer fluid. The slag would be replacing part of the molten salts. To compare these results, a conventional CSP plant has been used as a reference to identify the mass and energy flows.

This analysis is taken into consideration to evaluate the environmental impacts of the mention thermocline TES system for CSP plants, as well as, to identify some possible improvements in the selection and use of materials, focusing on revalorizing waste from industries with high environmental impact while reducing the quantity of materials needed for power generation, and leading to increase the sustainability associated with the implementation of these technologies.

2 General objective

- Perform the Life Cycle Assessment (LCA) of a concentrating solar power (CSP) plant that uses EAF steel slag as thermal energy storage material in a thermocline configuration and comparing it to a conventional CSP plant in terms of the environmental impacts associated to each one.

2.1 Specific objectives

- Establish a methodology to assign the impact points to by-products from the mining and metallurgical industry (case of study: EAF steel slag) as thermal storage materials, considering the standards from the ISO 14040-2006 and the ISO 14044-2006, and previous investigations.
- Identify the main opportunities associated to use the EAF steel slag as thermal storage material for the sustainability improvement of thermal storage systems in CSP plants, throughout the evaluation of its potential environmental impacts, and taking as a reference the United Nations' Sustainable Development Goals (SDGs).

3 Materials and methods

3.1 Description of the considered CSP plant

Four elements are required in CSP plants: concentrator, receiver, transport/storage media system, and power conversion device [3]. In this specific case of study, a solar power tower configuration was chosen, known as a central receiver that is the centre of all concentrating solar collectors. The solar tower use sun tracking mirrored solar dish collectors (heliostats) - spread over a large area - to reflect the sunlight directly onto the centrally located heat absorbing receiver, found at the top of the tower, from where molten salts are heated from 290 °C to 565 °C and then enter the thermal storage tank. Later, hot salts are pumped from the storage system to generate steam within a molten salt steam generator. Finally, the cooled salt is returned through the thermal storage system back to the receiver [7]. A scheme of this process -where the thermocline tank is incorporated in the tower- is shown in Figure 1.

Some of the considerations described by Gasa et al. [8] 2021 in the study: “*Life Cycle Assessment (LCA) of a Concentrating Solar Power (CSP) Plant in Tower Configuration with and Without Thermal Energy Storage (TES)*” are included in this research, as a manner to deepen previous related scenarios of a conventional CSP plant (two-tanks TES system). These considerations have also been taken into account in the definition of the TES system.

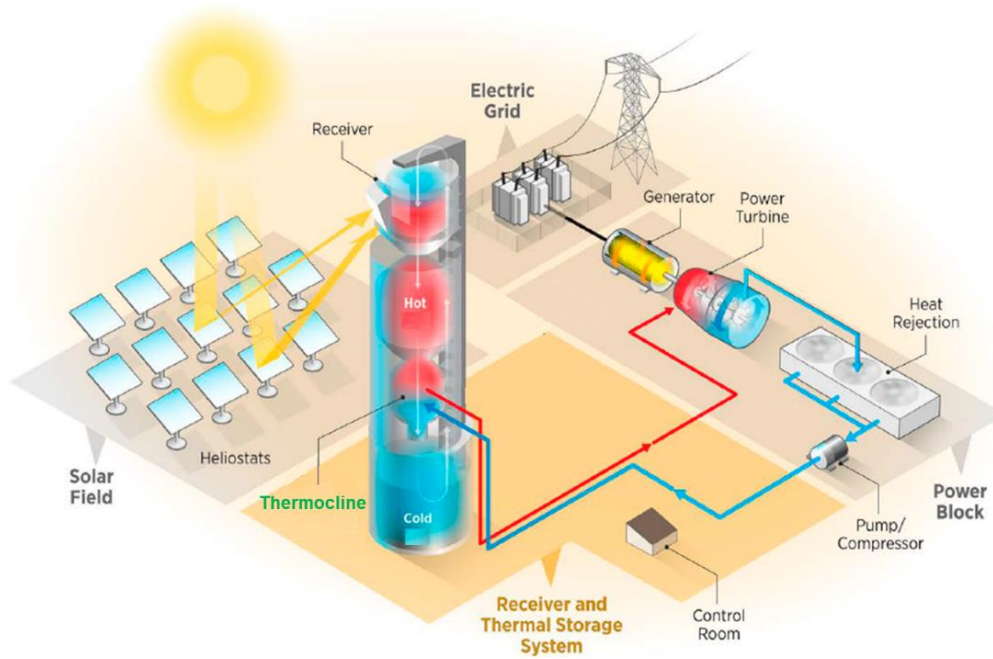


Figure 1. CSP tower with thermocline TES system. Adapted from: [9].

This research considers that the CSP plant was designed to operate 24 hours per day for most of the year (baseload configuration). The design of the baseload power plant aims to maintain a consistent electricity output throughout the entire day, maximizing the capacity factor of the plant on an annual basis. To accomplish this with solar energy as the primary input, the presence of a storage system is essential. This storage system must effectively manage solar transients, such as cloudy days, and provide the necessary energy for nighttime electricity production. Table 1 presents the specifications of the CSP tower plant considered in this study.

Table 1. Characteristics of the assessed CSP tower plant. Source: [8].

Characteristics	CSP plant considered	Units
Capacity, gross	120,8	MW
Capacity, net	110,0	MW
Number of heliostats	10.600	units
Solar field aperture area	1,5	km ²
Tower height	240	m
Receiver power level	690	MW
Direct normal irradiance	3.332	kWh/ (m ² . yr)
HTF mass (heat transfer fluid)	56.160	metric ton
Thermal energy storage capacity	5.330	MWh _{th}
Annual net electricity fed to the grid	776,24	GWh _{el}
Annual off-line electricity consumption	0,9	GWh/yr
Annual water consumption	64.250	m ³ /yr
Type of land use before this project	desert	--

3.2 Description of the TES system considered

The thermal energy storage system consists of the following elements:

- a) Nitrate salt inventory: molten nitrate salt (60 wt% NaNO_3 , 40 wt% KNO_3) as the heat transfer fluid and the thermal storage material (TESM), both.
- b) Thermocline tank: filled with EAF steel slag pebbles (packed-bed), also used for TES purposes.
- c) The molten salt circulation pumps.

In a thermocline tank system, Heat Transfer Fluid (HTF) flows through the TESH, as illustrated in Figure 2. This fluid usually reaches high temperatures (above $\sim 500\text{ }^\circ\text{C}$). During the energy input (charging step), hot fluid is injected at the top of the tank. The heat is transferred to the filler material and cold fluid is extracted from the bottom of the tank. Hence, three different zones appear: a hot zone at the top, a cold zone at the bottom and a zone with a large temperature gradient in the middle, called the thermocline. During the discharging step, cold fluid is injected at the bottom and hot fluid is extracted from the top. The same three zones appear. In both steps, the thermocline zone moves through the tank until it is partially or fully extracted [10].

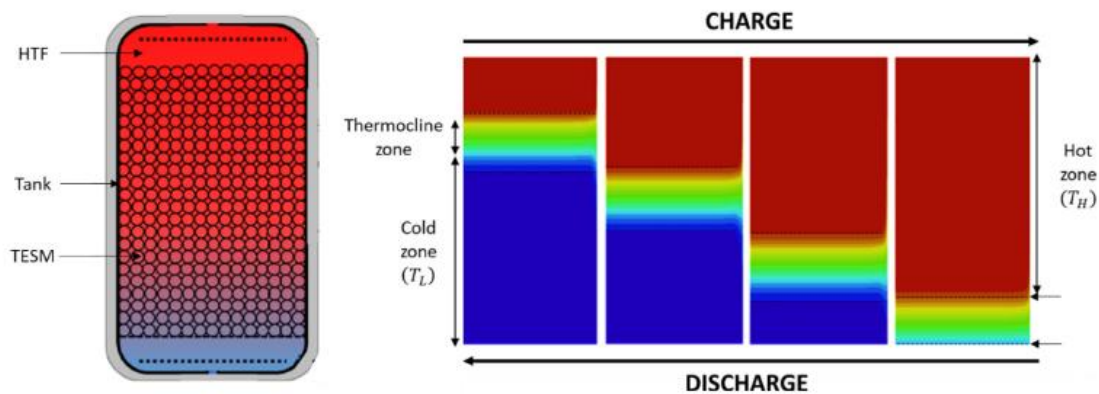


Figure 2. Thermocline tank working principle. Source: [10].

For the conservative design of the thermocline, the storage single-tank is fabricated with ASTM A-347H or ASTM A-321H carbon steel (the same materials of what a hot tank is made up in a conventional two-tanks configuration). Inside the tank, the vertical design molten salt circulation pumps are located. Molten salt steam generators typically consist of a series of shell and tube heat exchangers, comprising a preheater, an evaporator, a superheater, a reheater, and a steam drum. The tube side is dedicated to the high-pressure fluid (steam), while the shell side accommodates the low-pressure fluid (molten salt). To enhance the heat exchanger's reliability, the tubes are rolled and seal-welded to the tube-sheet. These components are primarily constructed from stainless steel, due to the operating temperature and potential corrosion concerns.

The plant storage capacity is considered as 17,5 equivalent hours at nominal conditions, this choice was made considering that the impacts generated throughout the plant useful life remain relatively unchanged when the storage capacity is further increased from 9 hours to 17,5 hours [7]. The combination of this storage capacity and simultaneous daytime production enables continuous electricity generation to meet baseload demand 24/7.

In this research, evaluating the impact of a hypothetical CSP plant that uses EAF steel slag as thermal storage material -in a thermocline TES system- entailed to compare with one CSP plant that uses a conventional molten salt storage system (Figure 3). This comparison was conducted by using the same technology but making the necessary changes related to the amount of material required in each TES configuration. Therefore, the conventional two tanks/molten salt TES system in a solar tower power plant configuration described by Gasa et al. [8] 2021 was also considered as a reference for this comparison work.

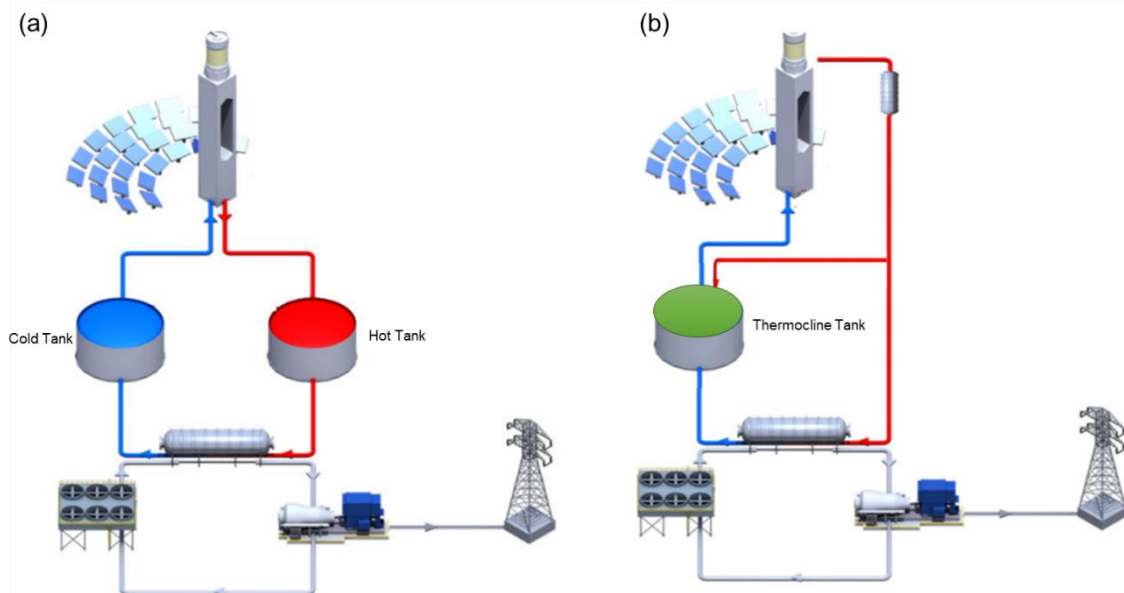


Figure 3. CSP Plant configurations: (a) Two-tanks TES system. (b) Thermocline TES System. Adapted from: [8].

3.2.1 EAF steel slag as thermal storage material

The possibility to use the EAF steel slag as a thermal storage material in a TES system have been addressed, confirmed, and documented in several investigations. These slags primarily consist of aluminium, calcium, iron, magnesium, and silicon oxides (Figure 4) [11]. By utilizing slag as TESM, the amount of material being sent to landfills can be reduced, leading to a decrease in air pollution during electricity generation and contributing to lower costs associated with climate change mitigation. Implementing a packed-bed storage solution based on EAF steel slag has the potential for success [12].



Figure 4. Pictures of raw EAF slags samples showing their general appearance. Source: [12].

The compatibility of EAF steel slag with molten salt is reported in [6], [12], [13] and [14], commenting that it could be used as filler material in a TES system in direct contact with the solar salt. Some properties of the selected thermal storage materials are summarized in the Table 2.

Table 2. Physical properties of selected heat storage materials. Sources: [5], [11] and [12].

Properties	Unit	Molten Salts	EAF Steel Slag
Density (ρ)	kg/m ³	900-2.600	3.400-3.700
Specific heat (C_p)	J/kg·K	1.500	912-1.360
Heat capacity per volume (ρC_p)	kJ/m ³ ·K	1.350-3.900	3.100-5.000
Thermal conductivity (λ)	W/m·K	0,15-2,0	1,41-1,75

A production process was developed to enhance the chemical and mechanical properties of gross steel slag. This process involves fine milling, compression, and sintering, resulting in improved mechanical resistance to thermal cycling of the final slag pebbles. Additionally, the chemical stability of the pebbles is enhanced, allowing them to withstand temperatures up to 1.000 °C under static test conditions in an air atmosphere. Furthermore, it has been observed that this production process effectively prevents the entrainment of fine solid steel particles and avoids any breakdown or alteration of the composition of the molten salts during cycling tests. These tests involved subjecting the slag pebbles, along with the molten salts, to temperature fluctuations ranging from 290 °C to 550 °C. This ensures the chemical stability of the slag during cycling conditions, thereby ensuring the operational stability and safety of the storage system [13]–[15].

Applying these processes to the gross steel slag is important since the use of raw slag aggregates would most likely be limiting the HTF velocity, since the poor shape homogeneity is susceptible to generate preferential pathways inside the thermocline tank, and generally induces problems linked to heat transfer and pressure drop [15].

Gil et al. [16] 2014 conducted a study to model a thermal energy storage unit using steel slag as the storage material in a packed-bed configuration. The modelled system was designed to operate within a temperature range of 120 °C - 650 °C. The researchers

modelled quasi-spherical pebbles with diameters of 1 cm and 5 cm to investigate the impact of this parameter on the overall system performance.

The comparison between the two pebble diameters revealed that the 1 cm pebbles exhibited a five-fold increase in exchange area compared to the 5 cm diameter pebbles. During the discharge operation, the temperature distribution within the packed-bed was analysed for both pebble diameters. The results showed that the use of smaller diameter pebbles resulted in a more abrupt temperature transition, indicating improved thermal behaviour for the storage application and an extension of the storage capacity [16]. Overall, this modelling study demonstrated the feasibility of utilizing steel slag as a suitable material for thermal energy storage applications, and furthermore this makes evident the necessity to apply the shaping processes to obtain small slag pebbles that could be successfully introduced in the thermocline tank.

Based on the above exposed, the Electric Arc Furnace steel slag (EAF slag) was chosen as the TESM that would help the thermocline effect, reducing the amount of molten salt commonly used in the conventional CSP plants.

4 LCA Methodology

4.1 Life cycle assessment

Life cycle assessment (LCA) is an analytical methodology used to measure the sustainability of a process or product by assessing the environmental impacts it generates throughout its life. This includes analysing discharges, waste, emissions into the atmosphere, and the consumption of raw materials and energy. The LCA considers the entire life cycle of the product or process from its origin, which includes the extraction and processing of raw materials, production, transport and distribution, use, maintenance, reuse, recycling, and disposal in landfill at the end of its useful life [17].

The ISO 14040 [18] and ISO 14044 [19] standards regulate the LCA methodology of a process or product, and the aim of compare competitive solutions. Therefore, this work has been achieved by following the mentioned standards, and consequently the assessment has been broken down into four phases:

1) The goal and scope definition, which is critical as it determines the outcome of the analysis. This phase sets the functional units, system boundaries, and limits to the analysis to identify where in the life cycle the study begins and ends and which processes within the technical system will be assessed.

2) The life cycle inventory analysis (LCI), which involves collecting data on the materials and energy flow within the considered system, including all environmentally important inputs and outputs.

3) The life cycle impact assessment (LCIA), where the evaluation of the potential environmental impacts stemming from all inputs and outputs obtained in the LCI takes place.

4) The final phase is interpretation, where all the results obtained are evaluated to draw conclusions. Overall, LCA provides a comprehensive approach to assess the sustainability of a product or process by considering its entire life cycle, from production to disposal (Figure 5).

Life cycle impact assessment (LCIA) plays a crucial role in interpreting LCA studies as it enables the conversion of emissions and resource extraction data into a concise set of environmental impact scores. This is achieved using characterization factors, which quantify the environmental impact per unit of stressor. While numerous impact evaluation methods exist, the present study relies on the ReCiPe 2016 and IPCC2013 GWP impact evaluation methods, which has been extracted from the Ecoinvent database [20], using the Product Sustainability Software GaBi [21].

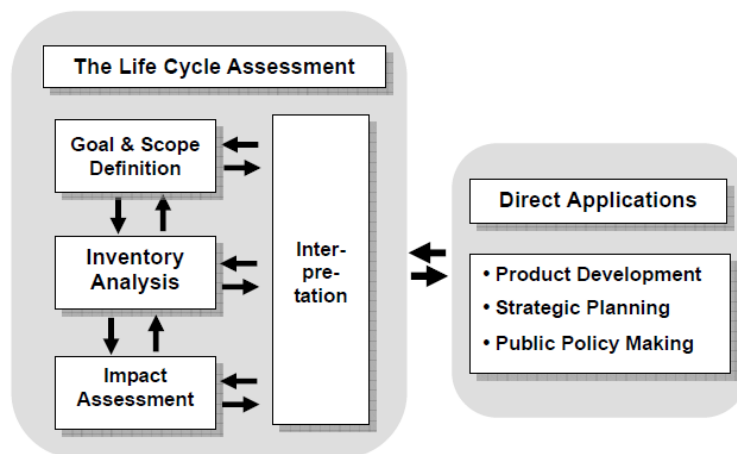


Figure 5. The relationship among the four phases in an LCA. Source: [17].

The ReCiPe method provides a framework for quantifying and evaluating the environmental impacts of human activities and processes [22]. Considering multiple impact categories, it utilizes characterization factors to convert the emissions and resource uses associated with a product or process into a common unit, allowing for the comparison and aggregation of different environmental impacts. Within the ReCiPe framework, environmental indicators are established at two levels: midpoint indicators and endpoint indicators. The ReCiPe incorporates three endpoint categories: human health, ecosystem quality, and resource availability (Figure 6). These indicators will be used to offer a comprehensive and robust approach for assessing environmental impacts across the various stages of a product or process life cycle.

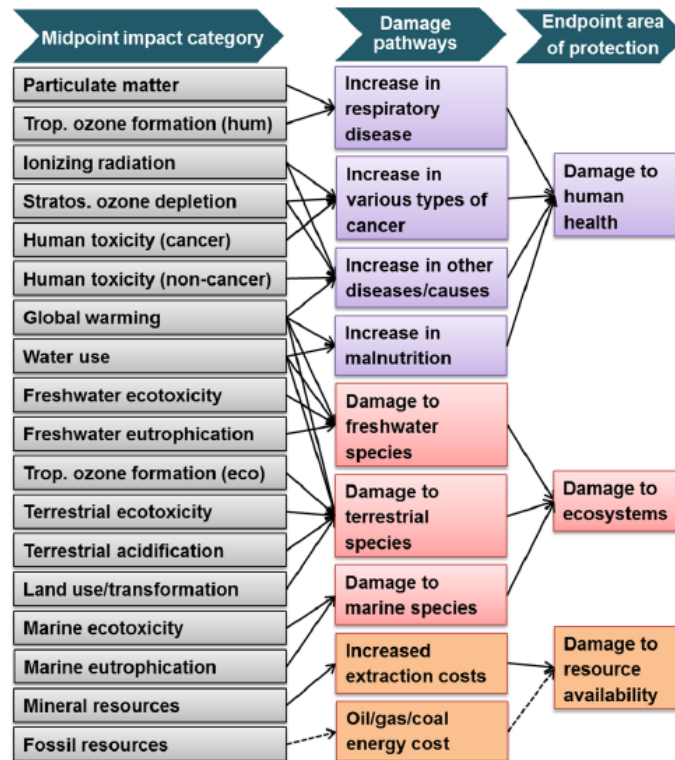


Figure 6. Impact categories that are covered in the ReCiPe2016 methodology. Source: [22].

On the other hand, the IPCC2013 GWP method focuses on climate change assessment and the characterization of the global warming potential (GWP) [8]. This metric allows for the estimation of the relative contribution to global warming caused by the atmospheric emissions of a specific greenhouse gas, in comparison to the emissions of 1 kg of carbon dioxide.

4.1.1 LCA Goal and scope

This research compares the environmental impacts of the conventional CSP storage technology (two tanks/molten salt) and those of the innovative storage (thermocline/steel slag and molten salt), in which the EAF steel slag material is used to replace part of the molten salt. The indicators obtained for each of the two configurations are evaluated from the LCA and identifying main opportunities to improve the sustainability of CPS systems by comparing the material and energy requirements in each configuration.

This comparison has been considered for the defined CSP plants, under the following operating conditions: a) baseload configuration, and b) thermal storage capacity equivalent to 17.5 hours during its estimated lifetime of 30 years.

4.1.2 Functional unit

In this study, the functional unit chosen was "1 kWh of net electricity fed to the grid". The global LCA results are presented in relation to this functional unit. By expressing the

environmental impacts per kWh, the results can be compared to other studies conducted using a similar approach.

4.1.3 System boundary

The scope of this study encompasses the "cradle-to-grave" perimeter, which covers the entire life cycle of the parts of a CSP tower plant. This includes assessing their impact in its construction, operation, and end-of-life phases. Regarding the end-of-life stage, it includes the transportation and disposal of waste materials.

Therefore, the system boundaries of the study (Figure 7) encompassed the following life-cycle phases:

- **Manufacturing phase:** This phase encompassed the acquisition of raw materials, construction of components, and procurement of building materials, as well as the energy required for on-site setup.
- **Operational phase:** This phase encompassed all activities associated with the operation of the plant, including grid electricity consumption, process water usage, and the procurement of materials necessary for proper functioning, such as water treatment chemicals.
- **End-of-life phase:** This phase encompassed the dismantling of plant components, demolition of buildings, and transportation of these materials to landfill sites and/or recycling sorting plants.

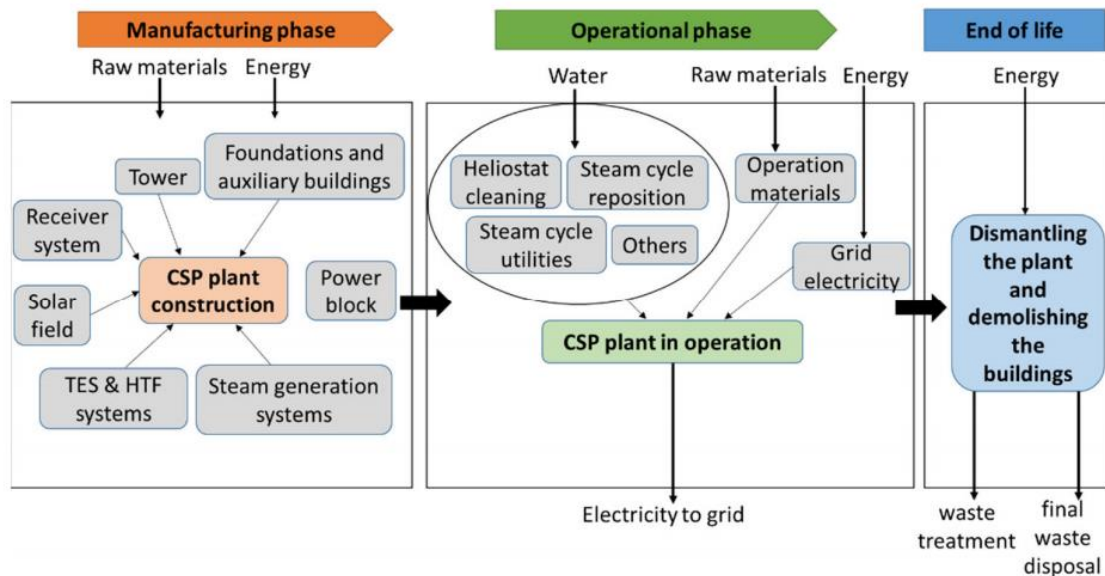


Figure 7. System boundary of a concentrating solar power (CSP) plant. Source: [8].

Even when all these phases are considered, the final results from the life cycle inventory analysis and the life cycle impact assessment will be shown placing in perspective the impact assessment of: the by-product, the TES systems and the CSP plant, in each

configuration. The consumptions of water and energy in the operational phase of the CSP plant are assuming not changing, as neither the consumption of energy in the end-of-life phase.

4.1.4 EAF steel slag perimeter: methodology to assign the impacts points

The precise delineation of the EAF steel slag perimeter is crucial: in this case the waste/by-product from one product system enters another product system as raw materials. The use of materials from one product system -disposed of as waste but collected and processed as raw materials in another product system- results in reduction of the environmental load of both product systems, this is called a multifunction system [5].

At this point, it is important to introduce to the Allocation's concept, which is a challenging aspect of an LCA study, involving the partitioning of input and output flows within the product system under examination. It is essentially the distribution of the environmental load created by unit processes in proportion to the product system being analysed [17].

Regarding to multifunction system, Figure 8 illustrates the two strategies of subdivision and system expansion in a simple and theoretical multifunctional process. This process comprises two distinct subprocesses that generate different products using the same raw material. In this example, only product A is used in the life cycle investigated, it provides an internally used function, while product B provides an external function. In this scenario, the allocation issue can be avoided through subdivision if detailed data regarding the functions produced, raw material demand, energy consumption, emissions, and waste can be obtained for each subprocess [23]. However, such comprehensive information is often unavailable, particularly when dealing with waste or by-products from industries.

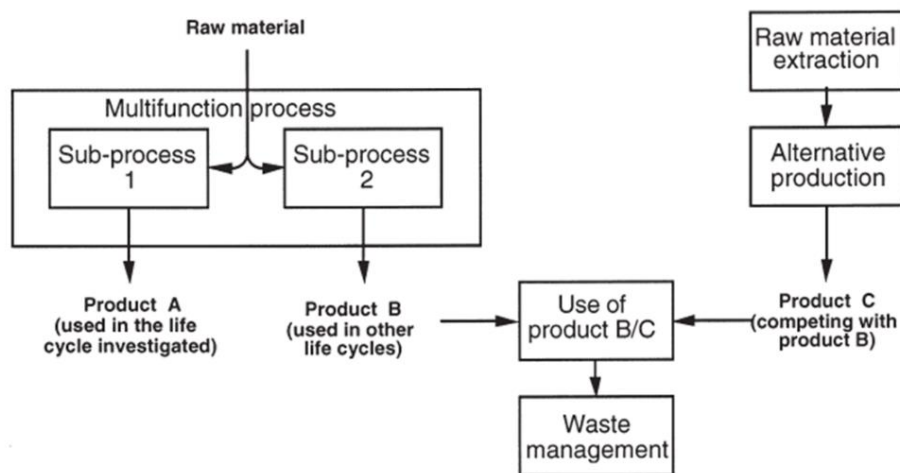


Figure 8. Theoretical multifunction process consisting of two separate sub-processes. Source: [23].

In summary, the allocation problem can be eliminated through subdivision if the multifunctional process consists only of single function subprocesses and environmental data is accessible for each of these subprocesses, which is not the case of the steel slag.

Nonetheless, the ISO 14041 Standard mentions in an informative annex that the recommendation to divide the multifunctional process into subprocesses applies not only when subdivision completely resolves the allocation problem, but also when it reduces the problem to some extent [23]. This suggests that the environmental burdens of each subprocess should only be allocated to the functions to which the respective subprocess contributes. Subprocesses that contribute to a single function can be directly allocated to that specific function. This approach helps alleviate the allocation problem when the multifunctional process involves physically separated subprocesses that do not contribute to all the functions.

From the guidelines about the environmental management in life cycle assessment - contained in the ISO 14044 [19] Standards- is known a stepwise procedure to allocate by partitioning the input or output flows of a product system between the product system under study and one or more other product systems [24]. The steps are the following:

- Step 1: wherever possible, allocation should be avoided by
 - ✓ system subdivision
 - ✓ system expansion
- Step 2: if allocation cannot be avoided try first to implement physical relationships to allocate.
- Step 3: where relevant physical relationships are not found, use the economical allocation methods.

Based on the established in the last paragraphs, the subdivision method has been applied to reduce the allocation problems by considering only the steel slag subprocess functions. That is how the multifunctional process considered in this investigation is split into monofunctional processes: 1) EAF steel fabrication, and 2) shaping of EAF steel slag to produce pack-bed filler (slag pebbles). The transition from one subprocess to other is specifically examined at the point where the production of inert waste flow concludes (this case: EAF steel manufacture process). At this stage, the steel slag is treated as a secondary primary material that is free from pollutants and can be readily processed. This approach promotes the use of secondary raw materials and prevents the duplication of impact assessments [5].

However, to fully address the remaining allocation problem associated to the impacts of EAF steel slag shaping to produce the slag pebbles, an alternative methodological approach needs to be employed since the purpose is not to hide the consequent environmental impacts. Thus, allocation is needed to determine how much environmental load should be distributed to the processes of raw material acquisition and manufacture (in a “cradle-to-gate” approach) [17].

To establish an appropriate allocation procedure, several studies have been reviewed but just few of them embraced the aim of this study. In most of them “mass allocation” and “economic allocation” are highlighted as the common procedures to deal with distributing the environmental impact related to the by-products from metals [25]–[28].

Allocation by mass is generally preferred when the economic value per unit of output between co-products is similar. This is since mass remains relatively constant over time, while market values subject to market fluctuations. Other important aspect is that ferroalloys are often best viewed as single, aggregated materials and, ideally, their environmental impacts will not be broken down to the constituent elements. Meanwhile, in economic (or market value) allocation, the market values of the outputs are averaged over a certain time; longer periods are recommended to reduce the impact of random price spikes and drops. It is recommended that a 10-year average is used; other time spans can be used so long as the price data represents economically current information that minimizes the effect of volatility [26].

The allocation method used by Chen et al. [27] 2010 is which suits the most to the approach and aims of the present study. Therefore, it has been taken in consideration to determine the environmental loads involves in the acquisition and shaping of the slag pebbles for the thermocline TES systems.

Following the criteria of splitting the multifunctional process above explained, the environmental system has been categorized into two types of processes. As it is shown in Figure 9, primary production processes are responsible for generating the main product as well as the by-products or waste. On the other hand, secondary processes focus on treating the by-products or waste to create a suitable product [27].

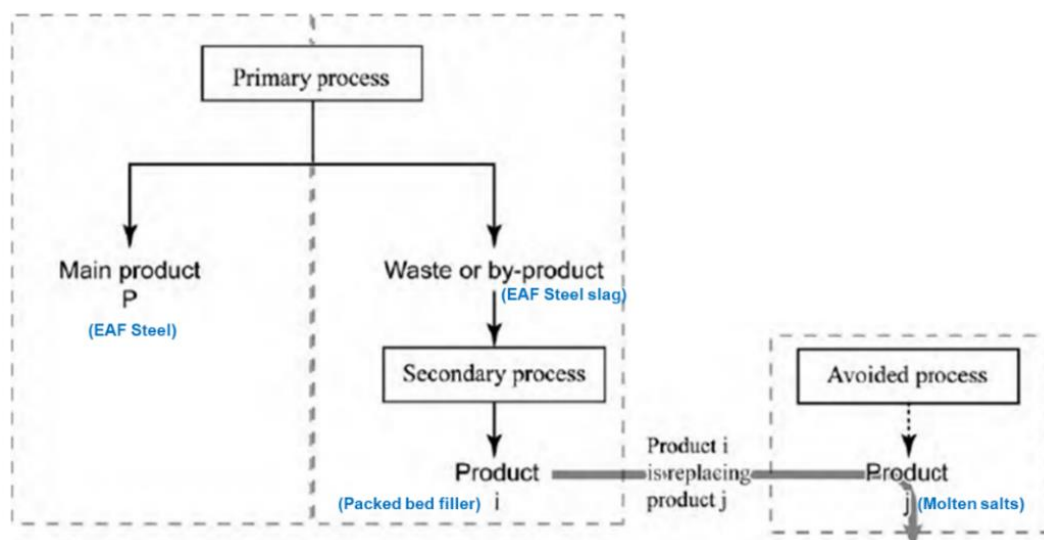


Figure 9. Description of the sub-systems involved in the study. Adapted from: [27].

Steel slag is co-produced with steel in an Electric Arc furnace. Thus, this is then considered as primary production process. After the electric arc furnace processing, steel slag needs to be fine milled, compressed, and sintered, to be suitable with its application as packed-bed filler [13] [14], these procedures belong to the secondary processes. The specific primary and secondary processes related to the production of EAF steel slag pebbles are outlined in Figure 10.

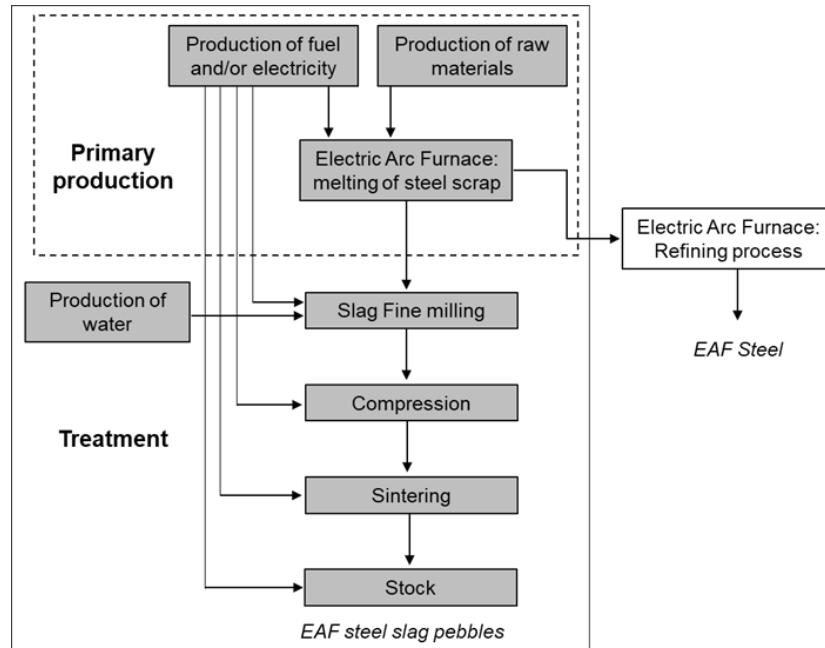


Figure 10. System boundaries of EAF steel slag-based packed bed filler. Adapted from: [27] and [15].

According to the establish, the secondary processes are fully allocated to the steel slag pebbles. Hence, the general presentation of inventory allocation for by-products (steel slag case) is as follows:

$$\vec{F}_{By-product} = C \cdot \vec{F}_{primary process} + \vec{F}_{secondary process} \quad (1)$$

Where, $\vec{F}_{By-product}$, $\vec{F}_{primary process}$ and $\vec{F}_{secondary process}$ refer to the flow inventories of environmental burdens of by-product, primary and secondary processes, respectively, and C is the allocation coefficient that differs whether the allocation method that is chosen.

As the transformation from the environmental inventory to the environmental impacts corresponds to a matrix A, that could be referred as a technology matrix [27], impacts for the steel slag pebbles can be expressed by Eq. (2).

$$\vec{I}_{By-product} = \vec{A} \left(c \cdot \vec{F}_{primary process} + \vec{F}_{secondary process} \right) \quad (2)$$

Where \vec{I}_I refers to environmental impacts of the by-product.

Eq. (2) is equivalent to Eq. (3) where the scalar C is extracted from the matrix product.

$$\vec{I}_{By-product} = c \cdot \vec{I}_{primary process} + \vec{I}_{secondary process} \quad (3)$$

Chen et al. [27] 2010, also mention that using the expansion method, and according to the defined system boundaries, shown in Figure 8, the environmental load of the by-product i can be expressed as:

$$\vec{F}_i = c \cdot \vec{F}_{primary process} + m_i \cdot \vec{F}_{secondary process} - m_j \cdot \vec{F}_{avoided process} \quad (4)$$

The approach of eq. (4) is the one taken into consideration in the present study to calculate the environmental impacts of using steel slag as TESM.

Multiple allocation methods can be employed within a single product system when different process sets and products are distinguishable. In the case of metals, mass allocation is preferable for characterizing upstream processes like mining and concentration, while economic allocation is more suitable for downstream processes like smelting and refining, especially when dealing with metal co-products [26]. However, it should be noted that economic allocation has the drawback of being susceptible to instability due to potential fluctuations in market prices [27]. Therefore, to simplify the system and making it more practical, in the present study only the mass allocation method will be employed to calculate the environmental impacts of the by-product.

The mass allocation coefficient C_m can be calculated as the mass ratio between main product and by-product:

$$C_m = \frac{m_{By-product}}{m_{Main product} + m_{By-product}} \quad (5)$$

Where $m_{By-product}$ and $m_{Main product}$ are the masses of by-product (steel slag) and of the main product (EAF steel), respectively.

4.1.5 Sources of environmental and economic data

It is being noticed that during the steelmaking process, EAF slags are generated as a by-product, with approximately 10-20% of slag produced per ton of steel [11]. In terms of production volumes, around 88 million tons of EAF slags are produced each year globally [15].

According to the European Slag Association [29], in 2010 the European EAF steel industry produced approximately 21,8 million tons of slag as a by-product of steel manufacturing. Around 76% of this steel slag was recycled and utilized in various applications such as construction aggregates and road materials. However, these sectors were unable to absorb the entire volume of generated slag, resulting in the remaining 24% being either landfilled (2,8 million tons) or stored on-site (2,2 million tons) [13].

In 2018, the production of steel slag in China was 110–120 million tons. Although the production is very huge, the utilization rate is less than 30%, and most of them are disposed of in landfills, which will cause serious environmental pollution problems. This constitute an issue that can be solve by the implementation of steel slag as the raw materials for sensible heat storage [30].

The slag landfills suppose a considerable source of air, water, and soil pollution, affecting adversely vegetation and fauna, and most especially human health. Considering the sintered slag is created from the waste provided by an Electric Arc Furnace -most common steel production in Europe- the thermocline tank with slag pebbles presents an additional way to revalorise the steelmaking slag and therefore, causes a potential reduction of the number and size of the slag landfills, improving the environmental situation. The slag pebble not only suits the necessary characteristic to be an interesting storage material as solid filler for thermocline tanks for CSP storage systems, but it also has a positive environmental impact reusing the steelmaking slag [14].

Filling this single-tank with a cost-effective solid material could replace a big amount of the molten salt inventory, which presents the highest global impact in TES system, achieving a more sustainable concept of thermal storage tank. Several authors have studied and compared single thermocline storage systems performance against the conventional two-tank storage showing potential cost reductions of 20-37% for the TES system. Besides, comparing between packed bed materials, the storage system using steel slag pebble can represent a cost reduction of 3,8% and 13% against the quartzite and taconite storage systems, respectively [13] [14].

Table 3, summarizes the comparison between these materials, highlighting the interest of the slag pebble material due to its higher ratio between heat capacity per volume of the slag and costs.

Table 3. Physical properties and price of slag pebbles, taconite, and quartzite rock. Sources: [12] [13].

Material	Density (kg/m ³)	Specific heat capacity (J/kg·K)	Heat capacity per volume (kJ/m ³ ·K)	Price	
				(€/t)	(€/kWh)
Taconite	3.200	800	2.560	178,73	--
Quartzite	2.500	830	2.075	10,01	--
EAF Steel slag Pebbles	2.850	970	2.765	80-100	1,14-1,17

4.1.6 Impact inventory

In this study, the environmental impacts related to materials and energy were assessed using the Ecoinvent database [20]. In most cases, data from the RoW (rest of the world) geographical area were selected.

4.1.7 Data inventory

As it was mentioned, the inventory of inputs and outputs for the conventional CSP tower plant with molten salt TES system was compiled using the real data from Gasa et al. [8] 2021, which is also utilized as a basis for constructing the inventory of the CSP tower plant with single-tank TES system. This entails to assume a hypothetical configuration where the values related to the among of materials required in the thermocline tank are obtained by scaling the values from the conventional plant inventory, in terms of the whole TES and HTF system.

The number of heliostats, solar tower height, and receiver thermal capacity in the CSP tower plant with single-tank configuration were assumed to be the same as in the conventional storage configuration. The main difference between these configurations lies in the type and quantity of materials that constitute the TES and HTF system, and in the fact that TESM must provide the same thermal storage capacity.

Regarding to the molten salt inventory, some authors mentioned that -in a thermocline configuration- up to 80% of the molten salt fluids can be replaced, without causing any drop in energy storage efficiency [31]. The typical filler materials used in the thermocline storage system – taconite and quartzite- effectively replaced approximately 67% of the salt that would typically be required in a two-tank system [5] [32]. Other example that can be mention is that a 32% reduction of the inventory of molten salt was achieved in a model of hybrid configuration TES system (2 thermocline tanks + 2 molten salt tanks) by using steel slag pebbles as filler material [13]. According to the explained, this research considers two scenarios of reduction for the total molten salt inventory:

- First scenario: To reduce by 60% the complete molten salt inventory of the TES and HTF systems respect to the conventional CSP plant.
- Second scenario: To reduce by 80% the complete molten salt inventory of the TES and HTF systems respect to the conventional CSP plant.

The inventory for the manufacturing stage of the two plants was divided into nine main groups, as illustrated in Figure 11. This division facilitated the completion of the inventory and allowed for a comprehensive analysis.

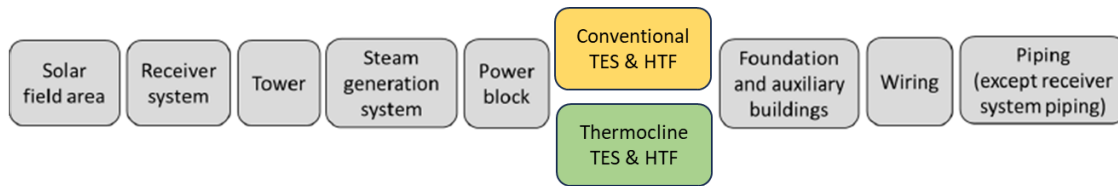


Figure 11. Classification of the processing of manufacturing inventory data. Adapted from: [8].

When sizing the thermocline TES and HTF system the quantities of materials needed are obtained by scaling volumetrically the material inventory of the conventional system, taking as inputs: i) the total thermal storage capacity of the CSP plant ($5.330 \text{ MWh}_{\text{th}}$), ii) the reduction scenarios of the total solar salt inventory, and iii) the volumetric thermal storage capacity of the new thermal storage material (steel slag pebbles). This constitutes a first sight over evaluating these CSP configurations, keeping the focus in the environmental loads assessment. Different scenarios -for instance: sizing the thermocline tank throughout numerical methods, accounting the discharging, and other related aspects affecting the total inventory of the CSP plant - will be addressed in further investigations.

Table 4 presents the inventory of materials of the CSP tower plant considered in this study. The consumptions of water and electricity the plant requires to function have been assuming to be the same as the conventional configuration, and also are included in this inventory. On the other hand, Annex 1 shows the detailed calculations of the materials required in the thermocline configurations.

Table 4. Materials and consumptions inventory for the two CSP plants. Adapted from: [8].

Component / Parameter	CSP Tower Plant	Unit
Solar field area components		
Flat glass coated	$1,1 \times 10^4$	t
Steel, low-alloyed	$3,6 \times 10^4$	t
Zinc coat, pieces	$2,7 \times 10^5$	m^2
Steel, unalloyed	$3,1 \times 10^3$	t
Lubricating oil	$5,7 \times 10^2$	t
Concrete	$9,5 \times 10^4$	m^3
Silicone product	$1,1 \times 10^2$	t
Electronics, for control units	$1,5 \times 10^2$	t
Receiver system		
Reinforcing steel	$1,7 \times 10^3$	t
Steel, chromium steel 18/8, hot rolled	$2,5 \times 10^2$	t
Silicone-based coating	7×10^{-1}	t
Refractory, basic	$2,6 \times 10^2$	t
Stone wool	$2,5 \times 10^1$	t
Tower		
Concrete	$1,9 \times 10^4$	m^3

Reinforcing steel	$3,6 \times 10^3$	t		
Excavation, hydraulic digger	$1,3 \times 10^4$	m^3		
Steam generation system				
Reinforcing steel	$8,2 \times 10^1$	t		
Steel, low-alloyed	$1,0 \times 10^2$	t		
Steel, chromium steel 18/8, hot rolled	$3,5 \times 10^2$	t		
Stone wool	$8,4 \cdot 10^{-2}$	t		
Glass fibre	2,3	t		
Power block (includes the power cycle components and the water tanks)				
Steel, chromium steel 18/8, hot rolled	$3,7 \times 10^2$	t		
Reinforcing steel	$3,0 \times 10^2$	t		
Steel, low-alloyed	$5,3 \times 10^2$	t		
Steel, unalloyed	$7,5 \times 10^1$	t		
Cast iron	$6,0 \times 10^{-2}$	t		
Copper	$1,8 \times 10^1$	t		
Aluminium	$6,2 \times 10^1$	t		
Stone wool	2,10	t		
Zinc coat, pieces	$6,1 \times 10^3$	m^2		
Foundation and auxiliary buildings				
Concrete	$9,7 \times 10^3$	m^3		
Reinforcing steel	$8,0 \times 10^2$	t		
Excavation, hydraulic digger	$7,4 \times 10^3$	m^3		
Building, hall	$4,8 \times 10^3$	m^2		
Wiring				
Cable	$1,9 \times 10^3$	km		
Piping (except receiver system piping)				
Reinforcing steel	$2,9 \times 10^2$	t		
Consumptions				
Grid electricity consumption (offline)	$9,0 \times 10^{-1}$	GWh/yr		
Water	$7,8 \times 10^4$	m^3/yr		
Chemicals for process water treatment	$7,1 \times 10^4$	kg/yr		
TES & HTF systems				
Component	Conventional TES & HTF	Thermocline TES & HTF		Unit
		First scenario	Second scenario	
Nitrate salts, for solar power application	$5,6 \times 10^4$	$2,24 \times 10^4$	$1,12 \times 10^4$	t
Steel slag pebbles	--	$1,71 \times 10^4$	$2,28 \times 10^4$	t
Steel, chromium steel 18/8, hot rolled	$1,2 \times 10^3$	$7,59 \times 10^2$	$6,12 \times 10^2$	t
Reinforcing steel	$1,4 \times 10^3$	$8,85 \times 10^2$	$7,14 \times 10^2$	t
Stone wool	$5,8 \times 10^2$	$3,67 \times 10^2$	$2,96 \times 10^2$	t

5 Results and discussion

5.1 Life cycle inventory analysis

Concerning to the estimation of the by-product impacts, it was found that using an average of 15% slag production per ton of EAF steel the C_m allocation factor reaches 0,13 (Eq. 5), for both chosen scenarios. In relation to the energy and water requirements to perform the secondary processes described in Figure 10, most of the consulted investigations [33]–[36] indicate the following values as representative, in terms of the expected consumptions for shaping the slag, and fully aligned with real data from manufacturing processes in the metallurgical industry:

- Energy consumption* (expressed per mass unit of the product to be treated):
 - Compression: 1 kWh/kg

- Sintering: 1,7 kWh/kg
 - * Ploted as the European attribute mix flow from ecoinvent database [20].
- Water consumption (expressed per mass unit of the product to be treated):
 - Fine milling: 1 m³/t

The energy involves in the milling and stock processes has not been considered since there is uncertainty about the real consumptions related to these stages. Therefore, the total consumptions associated to the shaping of the tank filler were calculated. In the first scenario, a total energy supply of 46.224 MWh is needed, and this value increases to 61.630 MWh in the second case. Meanwhile, the water needs supply maintains a 1:1 relationship with the quantity (in tons) of by-product to process in each scenario.

Figure 12 illustrates the material demand the TES and HTF systems components for each configuration. It is notable that in the first scenario the mass of molten salts still being higher compared to the quantity of steel slag estimated to enter into the single-tank system (22.400 t and 17.200 t, respectively). This can be explained as the result of the higher volumetric heat capacity (2.765 kJ/m³·K) and stored density (0,53 MWh_{th}/m³) the slag pebbles provide, allowing to reach the 5.330MWh_{th} storage capacity of the plant while reducing the materials intensity. Similar findings about storage characterization and properties of EAF steelmaking by-products for packed-bed filler purposes are found in the studies from Kocak et al. [37] 2020 and Kocak et al. [38] 2021.

On the other hand, the second scenario exhibits an increase of approximately twice the mass (22.827 t) of the slag pebbles respect to the conventional fluid. However, even when the by-product mass increment seems to be significant, the total inventory material continues reducing, this is because the system sizing was performed by volumetric scaling, and since the slag density is superior in relation to the salts, the second scenario inventory results in a lower mass material requirement compared to the first one (Annex I).

Summarizing, the total demand of materials decreases in both thermoclines' scenarios. The hybrid systems are characterized for having an improvement in the thermal storage density which involves a considerable materials reduction that ranges from 29,8% in the first scenario to 39,7% in the second one, respect to total inventory of the TES and HTF systems. The reported material savings are aligned with the fact that only one tank is required in the studied thermocline configuration.

The reduction in the material intensity is important since size changes in the TES and HTF systems can entail a reduction of the environmental impacts and affects positively the economic evaluation associated to the plant.

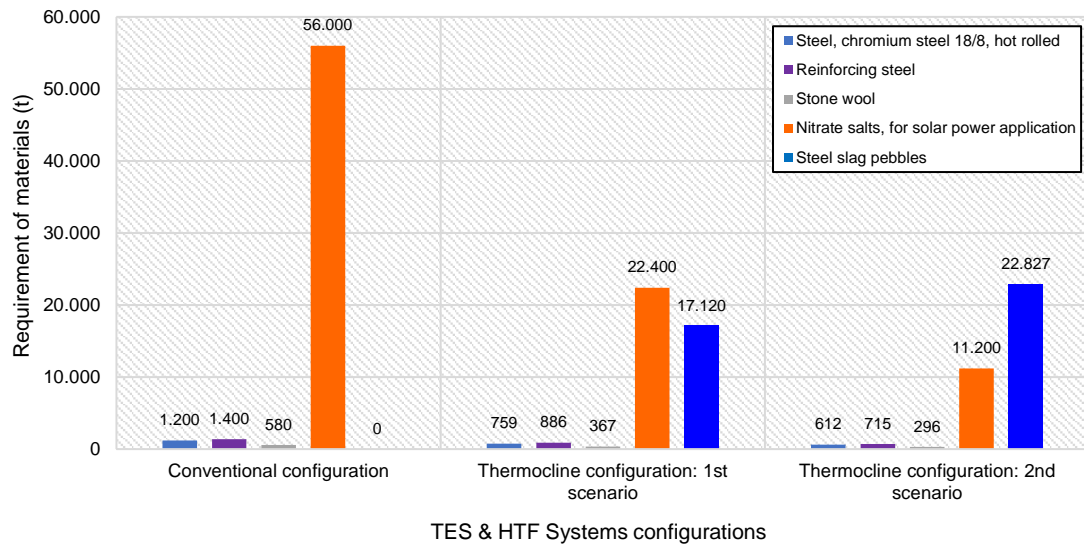


Figure 12. Materials demand associated to the TES and HTF Systems.

5.2 Life cycle impact assessment

The ReCiPe 2016 v1.1 E/A [20] was employed for quantifying and evaluating the environmental impacts. The following sections show a detailed account of the environmental impacts obtained from three perspectives, which include: the impact of the by-product, the study of each TES and HTF system, and the global impacts of the CSP plant.

To quantify the potential for global warming, the IPCC AR6 GWP 20 indicator was utilized [20], and its results are included in the overall perspective.

A scaling mechanism to optimally provide the results was incorporated in this research. In this sense, the by-product and the TES and HTF system perspectives are analysed considering the impacts per each kWh_{th} of the CSP Plant's thermal energy storage capacity. Meanwhile, to analyse the global impact of the entire CSP plant "1 kWh of net electricity fed to the grid" is used, as stated in Section 4.1.2.

5.2.1 By-product impacts estimation

According to the defined system boundaries, the environmental impacts of using steel slag as a TESM were calculated following the equation (4). The findings of the evaluated setups are presented in Table 5 (first scenario) and in Table 6 (second scenario). The own nature of the applied methodology to size the TES and HTF system already includes the subtraction of the impacts related to the avoided product (the molten salt).

Table 5. By-product impact calculation: First scenario.

	Primary process ($c_m \cdot \vec{F}_{primary\ process}$)	Secondary process ($m_i \cdot \vec{F}_{secondary\ process}$)		By-product (\vec{F}_l)
	Steel production	Energy consumption	Water consumption	Slag pebbles
Damage to human health (Impact / kWh _{th})	3,30E-01	4,05E-04	4,25E-05	3,30E-01
Damage to ecosystems (Impact / kWh _{th})	5,12E-04	2,03E-07	1,09E-07	5,13E-04
Damage to resource availability (Impact / kWh _{th})	36,17	1,53E-02	1,19E-02	36,20
*ReCiPe 2016 v1.1 (E/A) (Total impact / kWh_{th})	36,50	1,57E-02	1,19E-02	36,53

* The Table with the full impact categories related to the by-product is found in Annex III.

In both scenarios, the “bulk” of the data pertains to the environmental indicator of “Damage to resource availability”. This one contains two impacts categories: Fossil depletion and Metal depletion. The others environmental indicators (“Damage to human health” and “Damage to the ecosystems”) barely contributes to the by-product impact. It is notable that the primary process, which involves the EAF steel production and the EAF slag co-production, is the main contributor to the by-product total impact.

Table 6. By-product impact calculation: Second scenario.

	Primary process ($c_m \cdot \vec{F}_{primary\ process}$)	Secondary process ($m_i \cdot \vec{F}_{secondary\ process}$)		By-product (\vec{F}_l)
	Steel production	Energy consumption	Water consumption	Slag pebbles
Damage to human health (Impact / kWh _{th})	4,39E-01	5,40E-04	5,65E-05	4,40E-01
Damage to ecosystems (Impact / kWh _{th})	6,82E-04	2,71E-07	1,45E-07	6,83E-04
Damage to resource availability (Impact / kWh _{th})	48,3	2,04E-02	1,59E-02	48,34
*ReCiPe 2016 v1.1 (E/A) (Total impact / kWh_{th})	48,74	2,09E-02	1,59E-02	48,78

* The Table with the full impact categories related to the by-product is found in Annex III.

The impacts associated to the secondary process seem to be incipient respect to the total by-product impact. Even when some authors consider this type of furnace slags can be used directly in packed-bed filler applications (if regular shape is not needed) [38], the results show that preparing the EAF slag throughout the milling, compression and sintering processes does not contributes significantly to the slag pebbles impact.

To have a better understanding of the results associated to the by-product, a comparison contemplating the conventional TESM was performed.

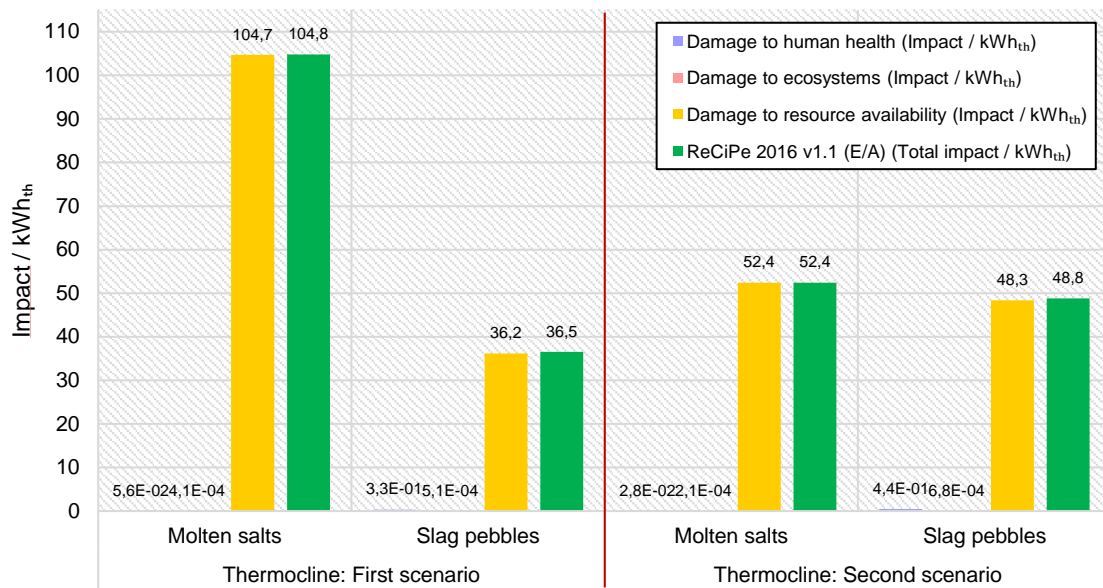


Figure 13. Impacts' comparison of the two TESM used in the thermocline configuration.

As it happened with the by-product, Figure 13 shows that the molten salts impact points are mainly assigned to the environmental indicator of “Damage to resource availability”. Besides, the molten salts impact reduction in the second scenario is consistent with its inventory reduction.

In the first scenario, the impact of the by-product represents 34% of the total molten salt’s impact. On the other hand, in the second scenario -which considers a smaller amount of salts- the slag pebbles impact represents 93% of the total salts impact points. Nevertheless, it can be concluded, in both scenarios the by-product impact is lower than the conventional TESM impact.

It is clear this comparison is not completely fair due to the molten salt impacts points were obtained by using a cradle-to-grave approach, meanwhile the by-product case incorporates the raw material acquisition and manufacture stages to calculate the impacts associated with the slag pebbles. Nevertheless, this comparison provides an initial sight of waste repurposing and reuse for TES applications and, the impact reduction reported is more promising when considers that -other way- in Europe at least 13% of the EAF steelmaking waste finishes in a landfill [29].

5.2.2 TES and HTF system impact estimation

The details of the TES and HTF systems plots for each configuration (conventional and thermocline) are shown in Annex II. After plotting the material inventory (processes and flows) for each scenario, the life cycle impacts associated to the TES and HTF system were calculated and their results are the following.

Table 7. Environmental impacts associated to the TES and HTF System

Configuration	Damage to human health (Impact / kWh _{th})	Damage to ecosystems (Impact / kWh _{th})	Damage to resource availability (Impact / kWh _{th})	*Total (Impact / kWh _{th})	Reduction (%)
Conventional	4,09E-01	1,18E-03	283,9	284	--
Thermocline: 1st scenario	5,56E-01	1,02E-03	154,9	155	45,4
Thermocline: 2nd scenario	6,04E-01	9,67E-04	111,9	112	60,6

* The Table with the full impact categories related to the TES and HTF system is found in Annex III.

Table 7 presents the impact points resulted from the studied configurations. Analogous to the by-product impact calculation, it is shown that the environmental indicator of “Damage to resource availability” has a wide dominium over the impact’s allocation. These can be linked to the fact that TES system require the implementation of intensive energy materials. The other environmental indicators also have marginal contributions.

However, a better look over these results makes contemplate that the “Damage to ecosystem” indicator continues decreasing when reducing the molten salt inventory in the thermoclines configurations, which can be considered as an indicator of sustainability increase.

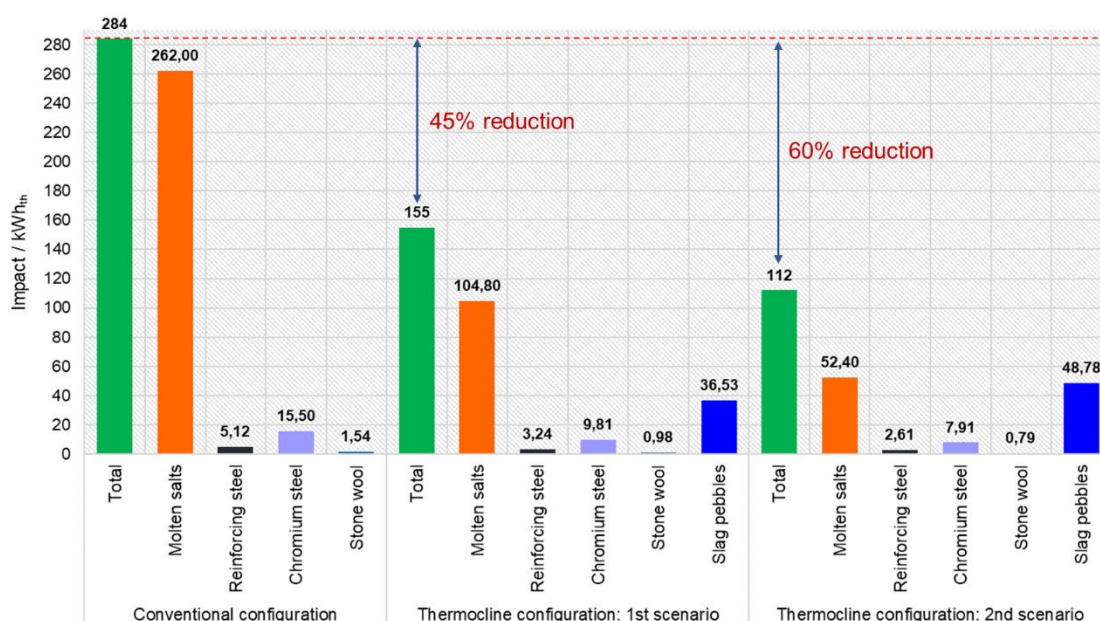


Figure 14. Comparison of the impacts from each TES and HTF component.

Figure 14 allows to analyse the reported results from the material’s inventory viewpoint. On it, each constituent material shows its contribution to the global TES and HTF system impact. As can be expected, the fewer requirement of materials entails to a diminution of the total environmental impacts in the thermocline configurations.

The use of the innovative storage system allows significant impact reductions: The total impact in the thermocline configurations displays a reduction of 45% in the first scenario and 60% in the second (respect to the total impact of the conventional TES and HTF system).

5.2.3 Global impact of the CSP Plant

As mentioned, the results of this section are exhibited in relation to the functional unit: “1 kWh of net electricity fed to the grid”. The details of the CSP plant plot are shown in the Annex II.

The global impacts of the concentrating solar power plant exhibit a behaviour analogous to those seen in the previous sections (Table 8). The intensity of materials required in a CSP plant somehow explain the highest density of impact allocation to the indicator of “Damage to the resource availability” for all scenarios. However, the decrease of this impact’s indicator is also notable in the single-tank configurations where the total inventory of materials was reduced as a consequence of using slag pebbles as TESM.

Table 8. Global environmental impacts associated to the CSP plant.

Configuration	Damage to human health (Impact / kWh)	Damage to ecosystems (Impact / kWh)	Damage to resource availability (Impact / kWh)	*Total (Impact / kWh)
Conventional	1,13E-03	1,20E-06	0,154	0,155
Thermocline: 1st scenario	1,17E-03	1,17E-06	0,124	0,126
Thermocline: 2nd scenario	1,18E-03	1,15E-06	0,115	0,116

* The Table with the full impact categories related to the CSP Plant is found in Annex III.

This information makes evident that reducing the total molten salt inventory by 60% induces a total impact reduction in the CSP plant of 19%. Likewise, when reducing the conventional fluid by 80% the global impacts present a reduction of 25% (Figure 15).

Gasa et al. [8] 2021 determined the relative contribution of each system of the CSP plant respect to the total impact points evaluated with the ReCiPe indicator, finding that in a two-tanks configuration the TES and HTF system have the highest impact (48%) over the others CSP plant systems.

As the present study uses as basis the inventory of materials from Gasa et al. [8] 2021, a simple extrapolation of their results was performed to gain insight of the potential impact reduction this innovative solution can bring to improve the CSP plant sustainability while revalorizing a waste product (Figure 16).

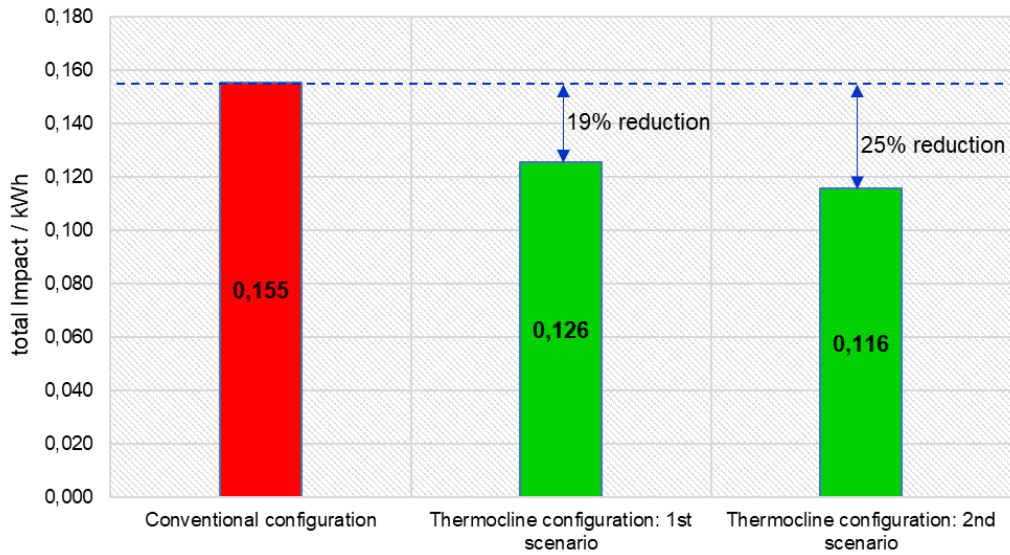


Figure 15. Global impact assessment of the CSP Plant.

Therefore, considering the global impact assessment of the CSP plant, it is estimated:

- In the first thermocline configuration, 19% of the impact reduction comports that the TES and HTF system would have a contribution of 38,8% respect to the others systems of the CSP plant.
- Meanwhile, the second thermocline configuration is equivalent to diminish the relative contribution of the TES and HTF system from 48% to 35,5%.

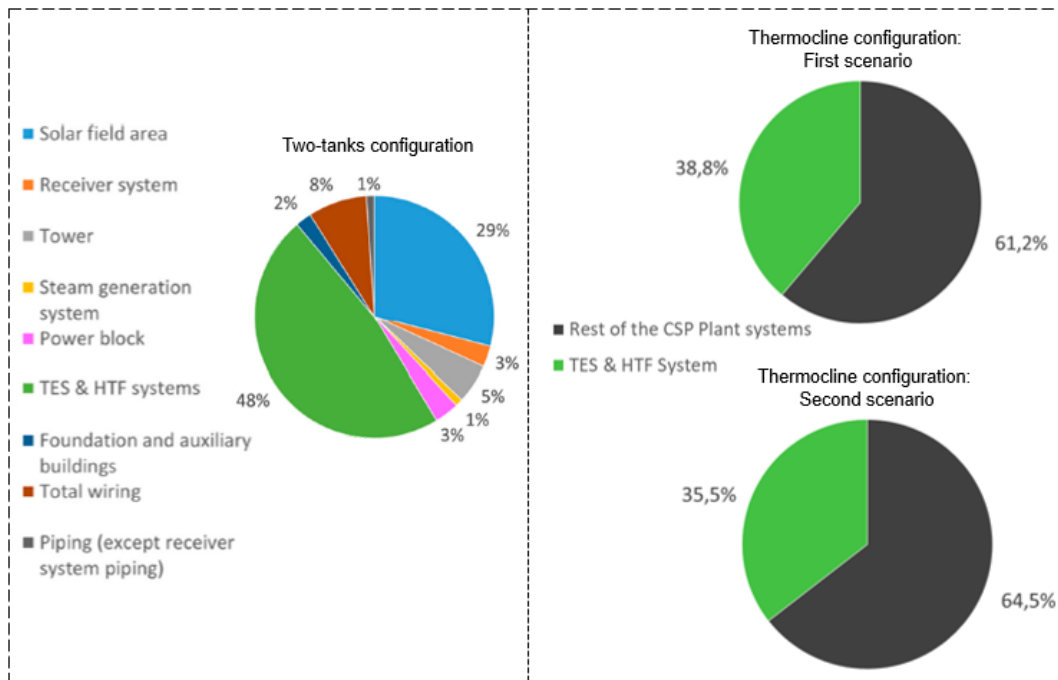


Figure 16. Comparative contribution of each TES and HTF System in the CSP plant. Adapted from: [8].

In other words, using the thermocline configuration, the contribution of the TES and HTF system to the total environmental impacts of the CSP Plant is reduced by 9,2% in the first scenario and by 12,5% in the second scenario.

Concerning to the impact calculated with the climate change indicator (IPCC GWP method) at 30 years, Table 9 shows which seems a little significant reduction of the total CO₂-equivalent emissions for both scenarios. Nonetheless, it is important to acknowledge that this reduction is all associated with the changes made in the TES and HTF system of the complete CSP Plant.

Some authors comment that the TES and HTF system is also known to be responsible of approximately 15% of the whole CSP Plant global warming potential and cumulative energy demand. Hence, the above estimated reductions will have corresponding effects on the whole plant environmental impacts [5].

Table 9. Total impact IPCC method: GW20 indicator per kWh of net produced electricity.

IPCC AR6 GWP 20 excl. biogenic CO ₂					
Configuration	Total emissions kg CO ₂ -Equiv/ kWh	Reduction (%)	Total net electricity fed to the grid (kWh)	Total (t CO ₂ - Equiv)	Reduction (t CO ₂ - Equiv)
Conventional	0,01201715	--	23.287.200.000	279.845,70	--
Thermocline: 1st scenario	0,01176682	2,08311652	23.287.200.000	274.016,19	5.829,51
Thermocline: 2nd scenario	0,01168432	2,76963335	23.287.200.000	272.095,00	7.750,70

Thus, the emissions associated to the TES and HTF system are re-calculated by considering the mentioned ratio of total emissions from the conventional CSP Plant (t CO₂-Equiv). The result indicates that 41.976,85 t CO₂-Equiv can be attributed to the thermal energy storage system of the plant. This approach allows to indicate that the reduction of the total emissions associated to the thermocline configurations ranges from 14% (first scenario) to 18% (second scenario).

It is worth noting that some exercises were conducted using the “CML2001 - Global Warming Potential method” [20] and similar results regarding climate change assessment and the characterization of the global warming potential were found.

5.3 Interpretation phase with a sustainability approach

According to the outcomes commented in the last sections, a general reduction in the negative environmental impacts of a conventional CSP plant can be achieved when compares to the thermocline hypothetical-alternative system by replacing one of the most impactful components in this type of plants (the molten salts), while revalorizing a high energy density material such as the EAF Steel slag.

The selected substitute material is obtained from a high energy demand industry, and - consequently- it has a significant environmental impact associated. This suggest that the defined methodology effectively distributes the environmental impacts of the by-product since its contributions to the impact accounting are mostly allocated to the “Damage to resource availability” impact category associated to the primary process.

Abokersh et al. 2021 comment that to obtain a circular and sustainable TES system is necessary integrating the reusing and recycling of alternative materials at the initial design of the CSP Plant. The evidence collected in the life cycle impact assessment provides a useful measure of how feasible is to implement the EAF slag pebbles into TES systems once it is clear that this packing material is abundant, energy efficient and (based on the results) sustainable enough for industrial scale applications. [39]

Additionally, the results illustrate that transforming this steelmaking industry waste into a product that can be repurposing as a thermal storage material do not contributes significantly to the accounting of environmental impacts. In fact, using steel slag as TESM would contribute to achieve some of the Sustainable Development Goals (SDGs) established by the United Nations [40], such as:

- SDG 7: Affordable and clean energy. A reduction of the material inventory would contribute to have a more cost-effective CSP Plant. The thermocline scenarios confirm that more sustainable and cleaner energy sources are achieved by reducing the global environmental impacts of the conventional CSP plant by up to 25%.
- SDG 9: Industry, Innovation, and Infrastructure. The reuse of EAF steel slag in thermal storage systems promotes innovation and the development of more sustainable infrastructures.
- SDG 12: Responsible production and consumption. The revalorization of slags as thermal storage materials contributes with a more responsible manner to resource management. This become evident in both thermocline scenarios where the impacts associated with the Metal depletion and Fossil depletion categories were the ones that decreased the most.
- SDG 13: Climate action: The findings indicate that using the steel pebbles for thermal storage, greenhouse gas emissions in the thermocline TES system can be reduced by up to 18% in comparison to the conventional TES system. The development of this technology would contribute to climate change mitigation.

6 Conclusion

The comparison of the concentrating solar power plant that uses EAF steel slag as thermal energy storage material in a thermocline configuration, conducted by the performance of a life cycle assessment, evidenced a significant reduction in the total demand of the material inventory respect to a conventional CSP plant, and also a decrease in the counting of the impact points.

The CSP plant global assessment reveal that the reduction in the molten salt inventory drives to a considerable decrease of the total environmental impacts of the plant, these reductions ranges from 19 to 25% in the studied scenarios. Thus, adopting the thermocline configurations in the CSP plant's TES system provides notable reductions in environmental impacts, mostly in terms of resources depletion and greenhouse gas emissions.

In both defined scenarios, the decrease in the environmental impacts of the TES and HTF system ranges from 45% (first) to 60% (second) in comparison to the conventional configuration. Regarding to the climate change impacts evaluation, the highest estimated reduction in emissions of the thermocline TES and HTF system reaches by up to 18% (7.750,70 t CO₂-Equiv).

The established method to allocate the by-product impact suggests primary process, linked to the "Damage to resource availability" category, is the main contributor to the environmental impact. On the other hand, the preparation of EAF slag via milling, compression, and sintering has fewer contributions to the slag pebbles impact.

The utilization of steel slag as a thermal storage material presents promising opportunities for sustainability improvement in CSP plants. The results demonstrate that repurposing steelmaking waste into thermal storage material is a practice aligns with several Sustainable Development Goals (SDGs), because this leads to: creating more cleaner energy solutions, promoting innovative technologies for green power generation, responsibly managing resources and contributing to climate change mitigation.

Further investigation should be performed to assess the subsequence stages in the life cycle of this packed-bed filler (when finishes its usefulness as TESM), and determine the impacts associated to its end-of-life phase. Other important aspects to abord in future research are: i) assess the packing factor respect to the size of the pebbles and its relation to the volume of salts to enter the tank, ii) sizing the thermocline tank (and the TES and HTF inventory) throughout numerical methods, iii) taking into consideration the efficiency ranges of this configurations, and iv) studying the slag pebbles impact from a cradle-to-grave approach and comparing it against the molten salts once again. Integrating the mentioned aspects will improve the comparative LCA analysis performed and diminishing the uncertainty associated with the taken assumptions.

7 References

- [1] N. Kincaid, G. Mungas, N. Kramer, M. Wagner, and G. Zhu, "An optical performance comparison of three concentrating solar power collector designs in linear Fresnel, parabolic trough, and central receiver," *Appl Energy*, vol. 231, pp. 1109–1121, Dec. 2018, doi: 10.1016/j.apenergy.2018.09.153.
- [2] T. Sueyoshi and M. Goto, "Comparison among three groups of solar thermal power stations by data envelopment analysis," *Energies (Basel)*, vol. 12, no. 13, 2019, doi: 10.3390/en12132454.
- [3] E. Oró, A. Gil, A. de Gracia, D. Boer, and L. F. Cabeza, "Comparative life cycle assessment of thermal energy storage systems for solar power plants," *Renew Energy*, vol. 44, pp. 166–173, Aug. 2012, doi: 10.1016/j.renene.2012.01.008.
- [4] A. Gil *et al.*, "State of the art on high temperature thermal energy storage for power generation. Part 1-Concepts, materials and modellization," *Renewable and Sustainable Energy Reviews*, vol. 14, no. 1. pp. 31–55, Jan. 2010. doi: 10.1016/j.rser.2009.07.035.
- [5] Y. Lalau, X. Py, A. Meffre, and R. Olives, "Comparative LCA Between Current and Alternative Waste-Based TES for CSP," *Waste Biomass Valorization*, vol. 7, no. 6, pp. 1509–1519, Dec. 2016, doi: 10.1007/s12649-016-9549-6.
- [6] Í. Ortega-Fernandez, J. Rodríguez-Aseguinolaza, A. Gil, A. Faik, and B. DAguanno, "New thermal energy storage materials from industrial wastes: Compatibility of steel slag with the most common heat transfer fluids," *Journal of Solar Energy Engineering, Transactions of the ASME*, vol. 137, no. 4, Aug. 2015, doi: 10.1115/1.4030450.
- [7] G. Gasa, C. Prieto, A. Lopez-Roman, and L. F. Cabeza, "Life cycle assessment (LCA) of a concentrating solar power (CSP) plant in tower configuration with different storage capacity in molten salts," *J Energy Storage*, vol. 53, Sep. 2022, doi: 10.1016/j.est.2022.105219.
- [8] G. Gasa, A. Lopez-roman, C. Prieto, and L. F. Cabeza, "Life cycle assessment (Lca) of a concentrating solar power (csp) plant in tower configuration with and without thermal energy storage (tes)," *Sustainability (Switzerland)*, vol. 13, no. 7, Apr. 2021, doi: 10.3390/su13073672.
- [9] M. Mehos *et al.*, "Concentrating Solar Power Gen3 Demonstration Roadmap," 2016. Accessed: Apr. 29, 2023. [Online]. Available: <https://www.nrel.gov/docs/fy17osti/67464.pdf>
- [10] D. Le Roux, R. Olivès, and P. Neveu, "Geometry optimisation of an industrial thermocline Thermal Energy Storage combining exergy, Life Cycle Assessment and Life Cycle Cost Analysis," *J Energy Storage*, vol. 55, Nov. 2022, doi: 10.1016/j.est.2022.105776.
- [11] Y. Wang, Y. Wang, H. Li, J. Zhou, and K. Cen, "Thermal properties and friction behaviors of slag as energy storage material in concentrate solar power plants,"

- Solar Energy Materials and Solar Cells*, vol. 182, pp. 21–29, Aug. 2018, doi: 10.1016/j.solmat.2018.03.020.
- [12] I. Ortega-Fernández, N. Calvet, A. Gil, J. Rodríguez-Aseguinolaza, A. Faik, and B. D’Aguanno, “Thermophysical characterization of a by-product from the steel industry to be used as a sustainable and low-cost thermal energy storage material,” *Energy*, vol. 89, pp. 601–609, Sep. 2015, doi: 10.1016/j.energy.2015.05.153.
- [13] J. López Sanz, F. Cabello Nuñez, and F. Zaversky, “Benchmarking analysis of a novel thermocline hybrid thermal energy storage system using steelmaking slag pebbles as packed-bed filler material for central receiver applications,” *Solar Energy*, vol. 188, pp. 644–654, Aug. 2019, doi: 10.1016/j.solener.2019.06.028.
- [14] F. Cabello Núñez, J. López Sanz, and F. Zaversky, “Analysis of steel making slag pebbles as filler material for thermocline tanks in a hybrid thermal energy storage system,” *Solar Energy*, vol. 188, pp. 1221–1231, Aug. 2019, doi: 10.1016/j.solener.2019.07.036.
- [15] N. Lopez Ferber, K. M. Al Naimi, J. F. Hoffmann, K. Al-Ali, and N. Calvet, “Development of an electric arc furnace steel slag-based ceramic material for high temperature thermal energy storage applications,” *J Energy Storage*, vol. 51, Jul. 2022, doi: 10.1016/j.est.2022.104408.
- [16] A. Gil *et al.*, “Characterization of a by-product from steel industry applied to thermal energy storage in Concentrated Solar Power,” 2014.
- [17] K.-M. Lee and A. Inaba, “Life Cycle Assessment Best Practices of ISO 14040 Series Ministry of Commerce, Industry and Energy Republic of Korea Asia-Pacific Economic Cooperation Committee on Trade and Investment,” Korea, 2004.
- [18] ISO, “ISO 14040 International Standard. Environmental management — Life cycle assessment — Principles and framework.,” *International Organization for Standardization (ISO), Geneva. Switzerland.*, 2006.
- [19] ISO, “International Organization for Standardization. (2006). Environmental management: life cycle assessment; requirements and guidelines (Vol. 14044). Geneva, Switzerland: ISO.,” *International Organization for Standardization*, vol. 2006, 2006.
- [20] G. Wernet, B. C., B. Steubing, J. Reinhard, E. Moreno-Ruiz, and B. Weidema, “Ecoinvent Version 3,” *Int J Life Cycle Assess*, vol. 21, no. 9, 2016.
- [21] Thinkstep, “GaBi Databases,” *GaBi Databases Upgrades & Improvements 2017 Edition*, 2017.
- [22] S. Huijbregts, Z. Steinmann, P. Elshout, and G. Stam, “ReCiPe 2016 v1.1 A harmonized life cycle impact assessment method at midpoint and endpoint level Report I: Characterization,” The Netherlands, 2017. [Online]. Available: www.rivm.nl/en

- [23] T. Ekvall and G. Finnveden, "Allocation in ISO 14041-a critical review," 2001. [Online]. Available: www.cleanerproduction.net
- [24] Agostini Alessandro, "Introduction to environmental impacts allocation," Roma, Nov. 2017.
- [25] J. X. Johnson, C. A. Mcmillan, and G. A. Keoleian, "Evaluation of life cycle assessment recycling allocation methods: The case study of aluminum Johnson et al. Evaluation of LCA allocation methods," *J Ind Ecol*, vol. 17, no. 5, pp. 700–711, 2013, doi: 10.1111/jiec.12050.
- [26] N. Santero and J. Hendry, "Harmonization of LCA methodologies for the metal and mining industry," *International Journal of Life Cycle Assessment*, vol. 21, no. 11, pp. 1543–1553, Nov. 2016, doi: 10.1007/s11367-015-1022-4.
- [27] C. Chen, G. Habert, Y. Bouzidi, A. Jullien, and A. Ventura, "LCA allocation procedure used as an incitative method for waste recycling: An application to mineral additions in concrete," *Resour Conserv Recycl*, vol. 54, no. 12, pp. 1231–1240, 2010, doi: 10.1016/j.resconrec.2010.04.001.
- [28] A. Dubreuil, S. B. Young, J. Atherton, and T. P. Gloria, "Metals recycling maps and allocation procedures in life cycle assessment," *International Journal of Life Cycle Assessment*, vol. 15, no. 6, pp. 621–634, Jul. 2010, doi: 10.1007/s11367-010-0174-5.
- [29] I. Ortega, A. Faik, A. Gil, J. Rodríguez-Aseguinolaza, and B. D'Aguanno, "Thermophysical Properties of a Steel-making by-product to be used as Thermal Energy Storage Material in a Packed-bed System," in *Energy Procedia*, Elsevier Ltd, May 2015, pp. 968–977. doi: 10.1016/j.egypro.2015.03.180.
- [30] I. Ortega-Fernández *et al.*, "Experimental validation of steel slag as thermal energy storage material in a 400 kWh prototype," in *AIP Conference Proceedings*, American Institute of Physics Inc., Jul. 2019. doi: 10.1063/1.5117741.
- [31] J. F. Hoffmann, T. Fasquelle, V. Goetz, and X. Py, "A thermocline thermal energy storage system with filler materials for concentrated solar power plants: Experimental data and numerical model sensitivity to different experimental tank scales," *Appl Therm Eng*, vol. 100, pp. 753–761, May 2016, doi: 10.1016/j.applthermaleng.2016.01.110.
- [32] H. Price *et al.*, "Advances in parabolic trough solar power technology," *Journal of Solar Energy Engineering, Transactions of the ASME*, vol. 124, no. 2, pp. 109–125, May 2002, doi: 10.1115/1.1467922.
- [33] K. He and L. Wang, "A review of energy use and energy-efficient technologies for the iron and steel industry," *Renewable and Sustainable Energy Reviews*, vol. 70. Elsevier Ltd, pp. 1022–1039, 2017. doi: 10.1016/j.rser.2016.12.007.
- [34] V. Kruzhanov and V. Arnhold, "Energy consumption in powder metallurgical manufacturing," *Powder Metallurgy*, vol. 55, no. 1, pp. 14–21, Feb. 2012, doi: 10.1179/174329012X13318077875722.

- [35] F. Zhao, J. Ogaldez, and J. W. Sutherland, "Quantifying the water inventory of machining processes," *CIRP Ann Manuf Technol*, vol. 61, no. 1, pp. 67–70, 2012, doi: 10.1016/j.cirp.2012.03.027.
- [36] R. de Souza Zanuto, A. Hassui, F. Lima, and D. A. Dornfeld, "Environmental impacts-based milling process planning using a life cycle assessment tool," *J Clean Prod*, vol. 206, pp. 349–355, Jan. 2019, doi: 10.1016/j.jclepro.2018.09.207.
- [37] B. Kocak and H. Paksoy, "Performance of laboratory scale packed-bed thermal energy storage using new demolition waste based sensible heat materials for industrial solar applications," *Solar Energy*, vol. 211, pp. 1335–1346, Nov. 2020, doi: 10.1016/j.solener.2020.10.070.
- [38] B. Kocak, A. I. Fernandez, and H. Paksoy, "Benchmarking study of demolition wastes with different waste materials as sensible thermal energy storage," *Solar Energy Materials and Solar Cells*, vol. 219, Jan. 2021, doi: 10.1016/j.solmat.2020.110777.
- [39] Z. Erregueragui, A. Tizliouine, L. Ouhaine, M. Chafi, and L. E. H. Omari, "Selection and performance evaluation of waste and by-product materials for thermal storage applications," *International Journal of Low-Carbon Technologies*, vol. 17, pp. 888–899, 2022, doi: 10.1093/ijlct/ctac060.
- [40] United Nations Development Programme, "Sustainable Development Goals (SDGs)," <https://www.undp.org/sustainable-development-goals>, 2023.

8 Annexes

8.1 Annex I: Calculation of materials required in the TES and HTF system inventory for thermocline configuration.

Step 1: Estimation of the total inventory of thermal storage materials in the thermocline configuration.

Input data:

A) Conventional configuration (two-tanks with molten salts)

- Total storage capacity = 5.330 MWh
- Molten salts density = 2,17 t/m³ (experimentally validated and within the range shown in the literature sources)
- Molten salt inventory = 56.000 t = 25.806,45 m³
- Assumption: All the molten salt in the TES and HTF system is used to obtain the plant's 5.530 MWh of thermal storage capacity
- Total inventory of thermal energy storage materials = 56.000 t = 25.806,45 m³

B) Thermocline configuration (single tank: molten salts + steel slag pebbles)

- Total storage capacity = 5.330 MWh
- Molten salts density = 2,17 t/m³ (experimentally validated and within the range shown in the literature sources)
- Steel slag pebbles density = 2,85 t/m³ (obtain from the literature)
- Steel slag pebbles heat capacity per volume (ρC_p) = 2765 kJ/m³·K = 7,6806x10⁻⁴ MWh/m³/K
- Average temperature of the thermocline tank = 420 °C = 693,15 K

First scenario: 60% reduction of the complete molten salt inventory.

Results:

- Total molten salt inventory = 25.806,45 m³ x 0,4 = 10.322,58 m³ = 22.400 t

- Molten salts storage capacity = $\frac{10.322,58 \text{ m}^3 \times 5.330 \text{ MWh}}{25.806,45 \text{ m}^3} = 2.132 \text{ MWh}$

- Steel slag pebbles storage capacity = 5.330 MWh – 2.132 MWh = 3.198 MWh

- Steel slag pebbles storage density = 7,6806x10⁻⁴ MWh/m³·K x 693,15 K = 0,53 MWh/m³

- Total steel slag pebbles inventory = $\frac{3.198 \text{ MWh}}{0,53 \text{ MWh/m}^3} = 6.007,07 \text{ m}^3 = 17.120 \text{ t}$

- Total inventory of thermal storage materials in the thermocline configuration = Total steel slag pebbles inventory + Total molten salt inventory

6.007,07 m³ + 10.322,58 m³ = 16.329,59 m³ (volume)

17.120 t + 22.400 t = 39.520 t (mass)

Second scenario: 80% reduction of the complete molten salt inventory.

Results:

- Total molten salt inventory = $25.806,45 \text{ m}^3 \times 0,2 = 5.161,29 \text{ m}^3 = 11.200 \text{ t}$
 - Molten salts storage capacity = $\frac{5.161,29 \text{ m}^3 \times 5.330 \text{ MWh}}{25.806,45 \text{ m}^3} = 1.066 \text{ MWh}$
 - Steel slag pebbles storage capacity = $5.330 \text{ MWh} - 1.066 \text{ MWh} = 4.264 \text{ MWh}$
 - Steel slag pebbles storage density = $7,6806 \times 10^{-4} \text{ MWh/m}^3 \cdot \text{K} \times 693,15 \text{ K} = 0,53 \text{ MWh/m}^3$
 - Total steel slag pebbles inventory = $\frac{4.264 \text{ MWh}}{0,53 \text{ MWh/m}^3} = 8.009,35 \text{ m}^3 = 22.826,65 \text{ t}$
 - Total inventory of thermal storage materials in the thermocline configuration = Total steel slag pebbles inventory + Total molten salt inventory
- $5.161,29 \text{ m}^3 + 8.009,35 \text{ m}^3 = 13.170,64 \text{ m}^3$ (volume)
- $11.200 \text{ t} + 22.826,65 \text{ t} = 34.026,65 \text{ t}$ (mass)

Note: calculations were performed using all decimals.

Step 2: Determination of the volumetric scale factor (VSF)

First scenario: 60% reduction of the complete molten salt inventory.

Results:

$$\text{Volumetric scale factor} = \frac{\text{Total inventory of thermal storage materials in the thermocline configuration}}{\text{Total inventory of thermal storage materials in the conventional configuration}}$$

$$\text{Volumetric scale factor} = \frac{16.329,59 \text{ m}^3}{25.806,45 \text{ m}^3} = 0,63$$

Second scenario: 80% reduction of the complete molten salt inventory.

Results:

$$\text{Volumetric scale factor} = \frac{\text{Total inventory of thermal storage materials in the thermocline configuration}}{\text{Total inventory of thermal storage materials in the conventional configuration}}$$

$$\text{Volumetric scale factor} = \frac{13.170,64 \text{ m}^3}{25.806,45 \text{ m}^3} = 0,51$$

Note: calculations were performed using all decimals.

Step 3: Scaling of all the material from the total TES and HTF system.

Even when the inventory from the total TES and HTF system is being express in mass units, the scaling was performed by using the volumetric scale factor (VSF), this is because of all these materials are used for volumetric (containment) and non-mass functions.

Table 10. Scaling the Thermocline TES and HTF system inventory from the conventional plant inventory

Scaling the values from the conventional plant inventory						
Component	Conventional TES & HTF inventory	Thermocline TES & HTF				Unit
		Volumetric scale factor	First scenario	Volumetric scale factor	Second scenario	
Steel, chromium steel 18/8, hot rolled	1.200,00	0,63	759,33	0,51	612,43	t
Reinforcing steel	1.400,00	0,63	885,88	0,51	714,51	t
Stone wool	580,00	0,63	367,01	0,51	296,01	t
Nitrate salts, for solar power application	56.000,00	--	22.400,00	--	11.200,00	t
Steel slag pebbles	--	--	17.120,00	--	22.826,65	t
Total	59.180,00		41.532,21		35.649,60	t
	Material requirement reduction		29,82		39,76	(%)

8.2 Annex II: Plots of processes and flows for the considered CSP Plants

CSP PLANT WITH CONVENTIONAL TES SYSTEM

Plante proceso Magnitudes de referencia
Se muestran los nombres de los procesos básicos.

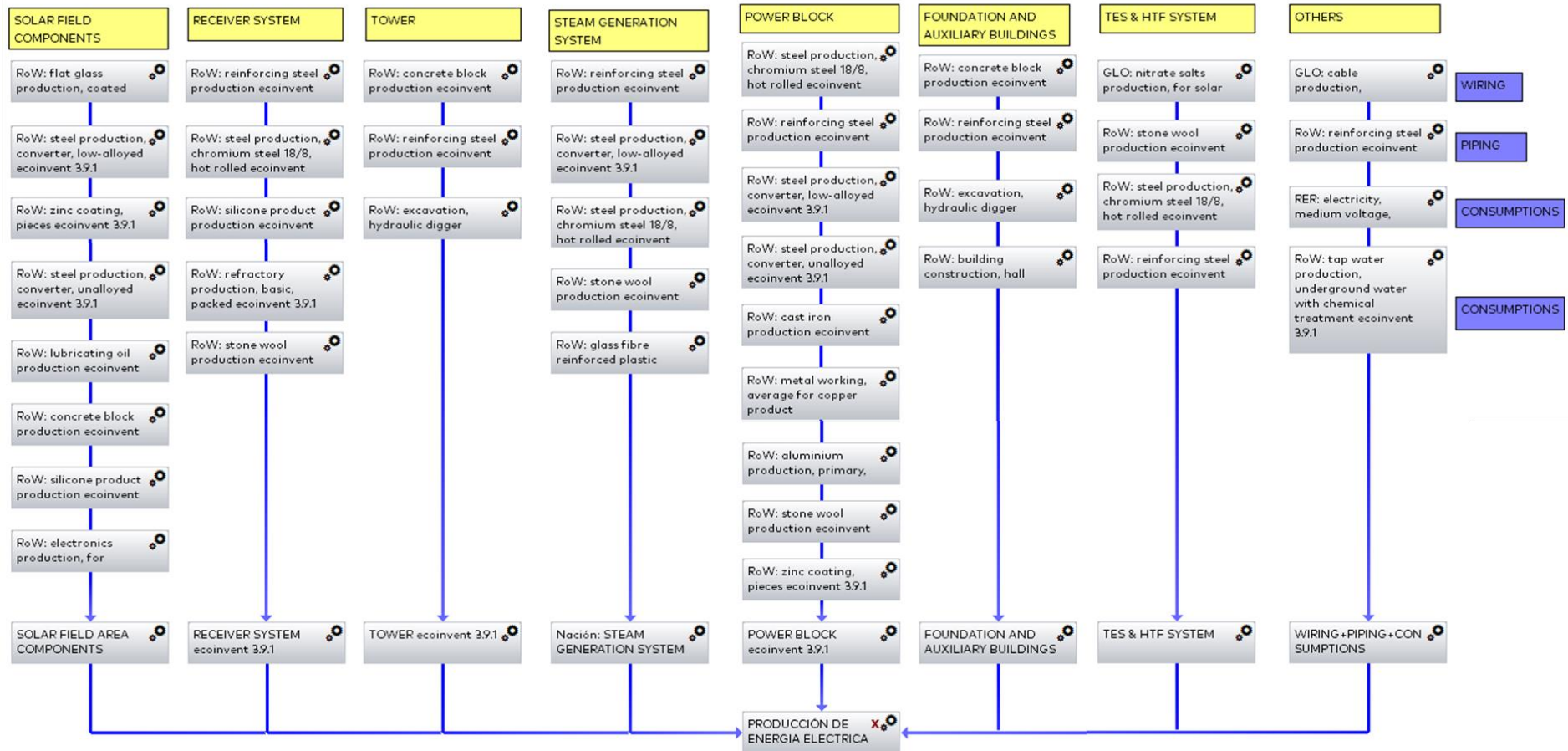


Figure 17. Plots of processes and flows used in the CSP Plant with a conventional TES and HTF System.

CSP PLANT WITH THERMOCLINE TES SYSTEM

Plante proceso Magnitudes de referencia
Se muestran los nombres de los procesos básicos.

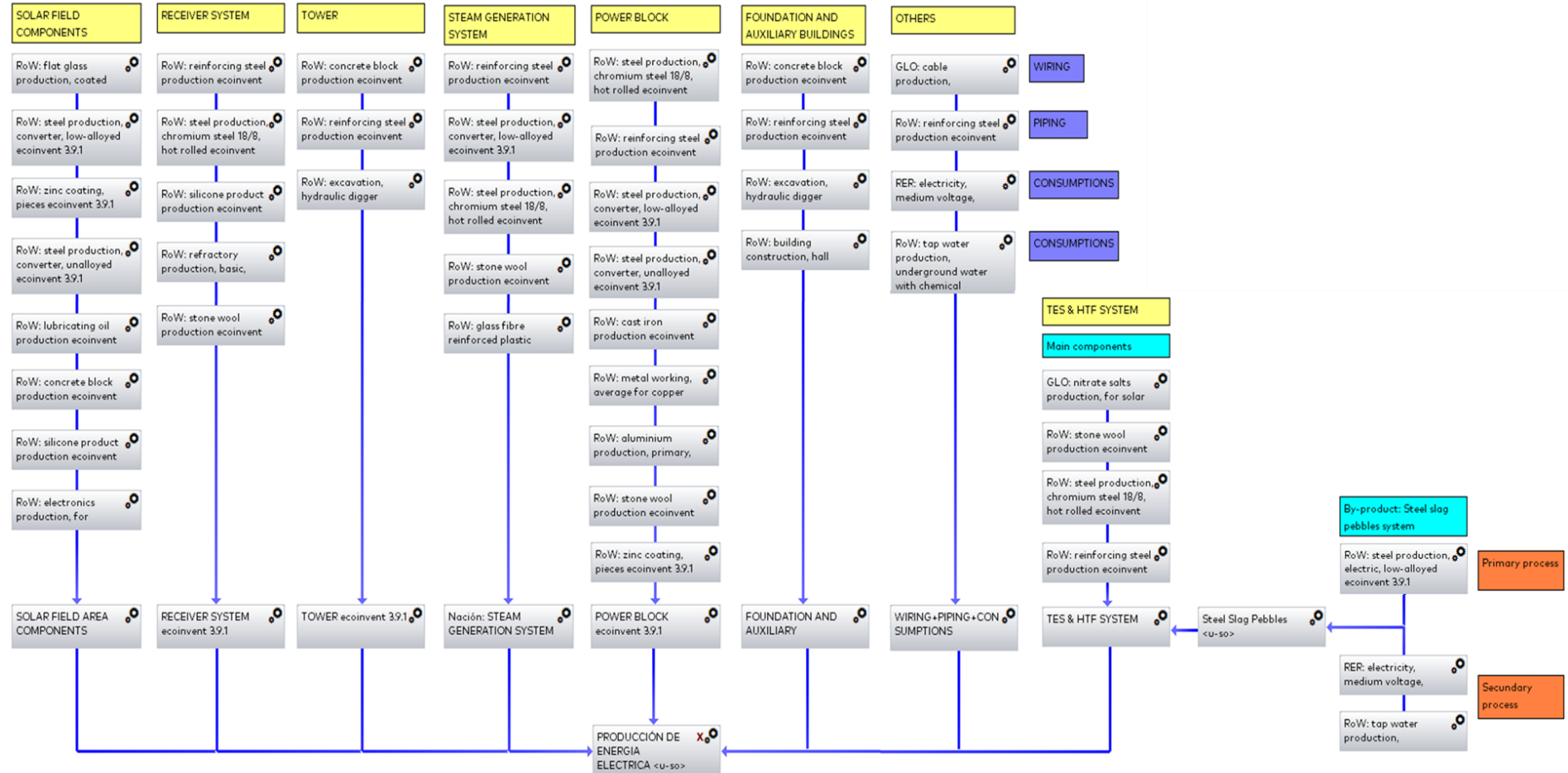


Figure 18. Plots of processes and flows used in the CSP Plant with a thermocline TES and HTF System.

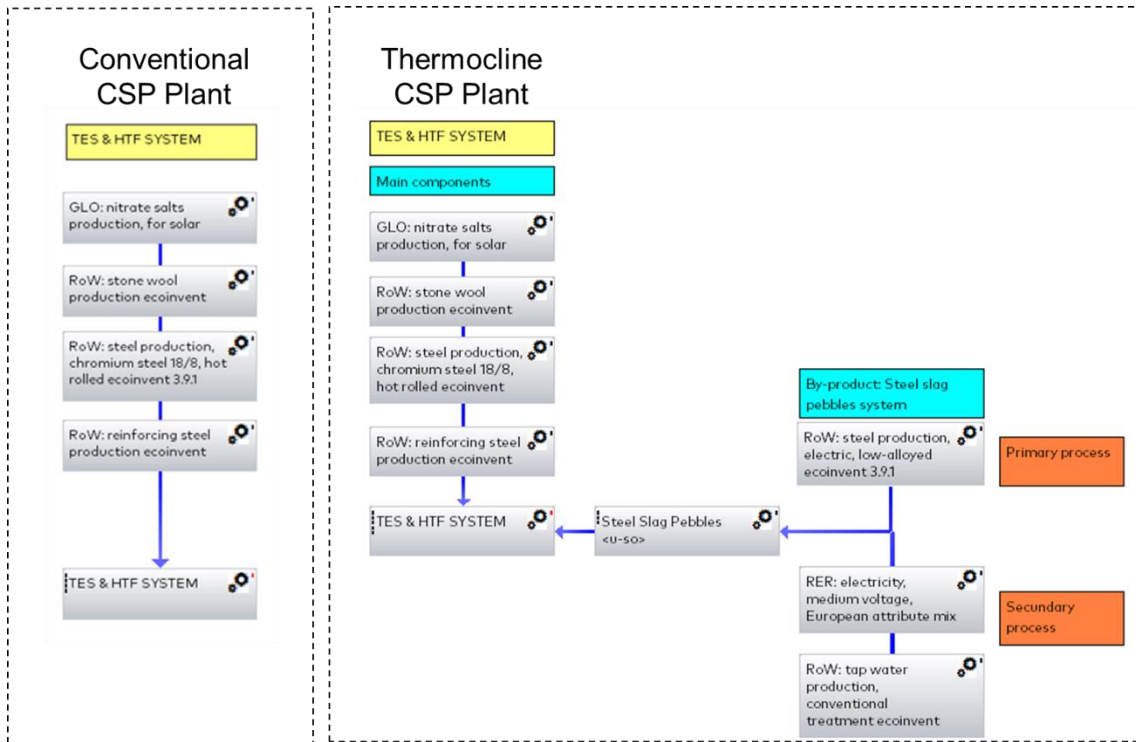


Figure 19. TES and HTF systems plots for each CSP Plant configuration.

8.3 Annex III: ReCiPe 2016 v1.1 (E/A) Complete impact categories data

Table 11. By-product complete impact categories data: First scenario.

Impact categories in ReCiPe 2016 v1.1 (E/A)	Primary process	Secondary process		By-product Impact
	Steel production * Cm (Impact/kWh _{th})	Energy consumption (Impact/kWh _{th})	Water consumption (Impact/kWh _{th})	Slag pebbles (Impact/kWh _{th})
ReCiPe 2016 v1.1 Endpoint (E) - Climate change Human Health, default, excl biogenic carbon [DALY]	2,22E-02	4,64E-06	6,33E-06	2,22E-02
ReCiPe 2016 v1.1 Endpoint (E) - Fine Particulate Matter Formation [DALY]	2,13E-03	5,21E-07	7,47E-07	2,13E-03
ReCiPe 2016 v1.1 Endpoint (E) - Freshwater Consumption, Human Health [DALY]	1,82E-05	5,64E-09	2,78E-06	2,10E-05
ReCiPe 2016 v1.1 Endpoint (E) - Human toxicity, cancer [DALY]	2,44E-01	5,18E-05	9,91E-06	2,44E-01
ReCiPe 2016 v1.1 Endpoint (E) - Human toxicity, non-cancer [DALY]	6,14E-02	3,48E-04	2,27E-05	6,18E-02
ReCiPe 2016 v1.1 Endpoint (E) - Ionizing Radiation [DALY]	5,46E-07	1,15E-10	9,86E-10	5,47E-07
ReCiPe 2016 v1.1 Endpoint (E) - Photochemical Ozone Formation, Human Health [DALY]	4,41E-06	3,73E-09	1,26E-09	4,41E-06
ReCiPe 2016 v1.1 Endpoint (E) - Stratospheric Ozone Depletion [DALY]	5,19E-07	1,40E-08	3,40E-10	5,33E-07
ReCiPe 2016 v1.1 Endpoint (E) - Climate change Freshw Ecosystems, default, [species.yr]	1,21E-09	2,53E-13	3,45E-13	1,21E-09
ReCiPe 2016 v1.1 Endpoint (E) - Climate change Terrest Ecosystems, default, [species.yr]	4,44E-05	9,28E-09	1,27E-08	4,44E-05
ReCiPe 2016 v1.1 Endpoint (E) - Freshwater Consumption, Freshw Ecosystems [species.yr]	1,42E-11	4,42E-15	2,18E-12	1,64E-11
ReCiPe 2016 v1.1 Endpoint (E) - Freshwater Consumption, Terrest Ecosystems [species.yr]	1,10E-07	3,43E-11	1,69E-08	1,27E-07
ReCiPe 2016 v1.1 Endpoint (E) - Freshwater ecotoxicity [species.yr]	5,32E-05	2,15E-08	8,97E-09	5,32E-05
ReCiPe 2016 v1.1 Endpoint (E) - Freshwater Eutrophication [species.yr]	6,03E-07	7,10E-10	1,36E-10	6,04E-07
ReCiPe 2016 v1.1 Endpoint (E) - Land use [species.yr]	2,44E-07	1,07E-10	7,82E-11	2,44E-07
ReCiPe 2016 v1.1 Endpoint (E) - Marine ecotoxicity [species.yr]	1,71E-05	1,18E-08	2,59E-09	1,71E-05
ReCiPe 2016 v1.1 Endpoint (E) - Marine Eutrophication [species.yr]	1,05E-10	2,44E-13	2,67E-14	1,05E-10
ReCiPe 2016 v1.1 Endpoint (E) - Photochemical Ozone Formation, Ecosystems [species.yr]	6,81E-07	5,36E-10	1,82E-10	6,82E-07

ReCiPe 2016 v1.1 Endpoint (E) - Terrestrial Acidification [species.yr]	1,03E-06	4,64E-10	4,42E-10	1,03E-06
ReCiPe 2016 v1.1 Endpoint (E) - Terrestrial ecotoxicity [species.yr]	3,95E-04	1,59E-07	6,65E-08	3,95E-04
ReCiPe 2016 v1.1 Endpoint (E) - Fossil depletion [\$]	27,70	1,50E-02	1,16E-02	27,73
ReCiPe 2016 v1.1 Endpoint (E) - Metal depletion [\$]	8,47	2,78E-04	2,81E-04	8,47
ReCiPe 2016 v1.1 (E/A), excl biogenic carbon. (Impact/kWh_{th})	36,50	1,57E-02	1,19E-02	36,53

Table 12. By-product complete impact categories data: Second scenario.

Impact categories in ReCiPe 2016 v1.1 (E/A)	Primary process	Secondary process		By-product Impact
	Steel production * Cm (Impact/kWh _{th})	Energy consumption (Impact/kWh _{th})	Water consumption (Impact/kWh _{th})	Slag pebbles (Impact/kWh _{th})
ReCiPe 2016 v1.1 Endpoint (E) - Climate change Human Health, default, excl biogenic carbon [DALY]	2,96E-02	6,19E-06	8,43E-06	2,96E-02
ReCiPe 2016 v1.1 Endpoint (E) - Fine Particulate Matter Formation [DALY]	2,84E-03	6,95E-07	9,96E-07	2,84E-03
ReCiPe 2016 v1.1 Endpoint (E) - Freshwater Consumption, Human Health [DALY]	2,42E-05	7,52E-09	3,70E-06	2,79E-05
ReCiPe 2016 v1.1 Endpoint (E) - Human toxicity, cancer [DALY]	3,25E-01	6,90E-05	1,32E-05	3,25E-01
ReCiPe 2016 v1.1 Endpoint (E) - Human toxicity, non-cancer [DALY]	8,19E-02	4,64E-04	3,02E-05	8,24E-02
ReCiPe 2016 v1.1 Endpoint (E) - Ionizing Radiation [DALY]	7,28E-07	1,54E-10	1,31E-09	7,29E-07
ReCiPe 2016 v1.1 Endpoint (E) - Photochemical Ozone Formation, Human Health [DALY]	5,88E-06	4,97E-09	1,68E-09	5,89E-06
ReCiPe 2016 v1.1 Endpoint (E) - Stratospheric Ozone Depletion [DALY]	6,92E-07	1,87E-08	4,54E-10	7,11E-07
ReCiPe 2016 v1.1 Endpoint (E) - Climate change Freshw Ecosystems, default, excl biogenic carbon [species.yr]	1,61E-09	3,38E-13	4,60E-13	1,61E-09
ReCiPe 2016 v1.1 Endpoint (E) - Climate change Terrest Ecosystems, default, excl biogenic carbon [species.yr]	5,91E-05	1,24E-08	1,69E-08	5,91E-05
ReCiPe 2016 v1.1 Endpoint (E) - Freshwater Consumption, Freshw Ecosystems [species.yr]	1,90E-11	5,89E-15	2,90E-12	2,19E-11
ReCiPe 2016 v1.1 Endpoint (E) - Freshwater Consumption, Terrest Ecosystems [species.yr]	1,47E-07	4,57E-11	2,25E-08	1,70E-07
ReCiPe 2016 v1.1 Endpoint (E) - Freshwater ecotoxicity [species.yr]	7,10E-05	2,87E-08	1,20E-08	7,10E-05

ReCiPe 2016 v1.1 Endpoint (E) - Freshwater Eutrophication [species.yr]	8,04E-07	9,47E-10	1,81E-10	8,05E-07
ReCiPe 2016 v1.1 Endpoint (E) - Land use [species.yr]	3,25E-07	1,43E-10	1,04E-10	3,25E-07
ReCiPe 2016 v1.1 Endpoint (E) - Marine ecotoxicity [species.yr]	2,27E-05	1,57E-08	3,45E-09	2,27E-05
ReCiPe 2016 v1.1 Endpoint (E) - Marine Eutrophication [species.yr]	1,40E-10	3,26E-13	3,56E-14	1,40E-10
ReCiPe 2016 v1.1 Endpoint (E) - Photochemical Ozone Formation, Ecosystems [species.yr]	9,08E-07	7,14E-10	2,42E-10	9,09E-07
ReCiPe 2016 v1.1 Endpoint (E) - Terrestrial Acidification [species.yr]	1,38E-06	6,18E-10	5,89E-10	1,38E-06
ReCiPe 2016 v1.1 Endpoint (E) - Terrestrial ecotoxicity [species.yr]	5,26E-04	2,12E-07	8,86E-08	5,26E-04
ReCiPe 2016 v1.1 Endpoint (E) - Fossil depletion [\$]	37,00	2,00E-02	1,55E-02	37,04
ReCiPe 2016 v1.1 Endpoint (E) - Metal depletion [\$]	11,30	3,70E-04	3,75E-04	11,30
ReCiPe 2016 v1.1 (E/A), excl biogenic carbon. (Impact/kWh_{th})	48,70	2,09E-02	1,59E-02	48,78

Table 13. Complete impact categories data: Conventional TES and HTF System

Impact categories in ReCiPe 2016 v1.1 (E/A)	Conventional configuration				
	Total	Molten salts	Reinforcing steel	Chromium steel 18/8	Stone wool
ReCiPe 2016 v1.1 Endpoint (E) - Climate change Human Health, default, excl biogenic carbon [DALY]	4,72E-02	3,86E-02	2,55E-03	5,38E-03	6,55E-04
ReCiPe 2016 v1.1 Endpoint (E) - Fine Particulate Matter Formation [DALY]	6,72E-03	5,34E-03	2,50E-04	1,04E-03	8,77E-05
ReCiPe 2016 v1.1 Endpoint (E) - Freshwater Consumption, Human Health [DALY]	3,65E-05	2,29E-05	3,29E-06	9,50E-06	7,69E-07
ReCiPe 2016 v1.1 Endpoint (E) - Human toxicity, cancer [DALY]	2,55E-01	2,93E-02	4,57E-02	1,80E-01	6,19E-04
ReCiPe 2016 v1.1 Endpoint (E) - Human toxicity, non-cancer [DALY]	9,99E-02	6,78E-02	8,25E-03	2,16E-02	2,30E-03
ReCiPe 2016 v1.1 Endpoint (E) - Ionizing Radiation [DALY]	1,35E-06	6,81E-07	1,09E-07	5,25E-07	3,20E-08
ReCiPe 2016 v1.1 Endpoint (E) - Photochemical Ozone Formation, Human Health [DALY]	1,23E-05	1,05E-05	5,27E-07	1,10E-06	1,35E-07
ReCiPe 2016 v1.1 Endpoint (E) - Stratospheric Ozone Depletion [DALY]	2,33E-06	1,99E-06	7,37E-08	2,49E-07	1,62E-08
ReCiPe 2016 v1.1 Endpoint (E) - Climate change Freshw Ecosystems, default, excl biogenic carbon [species.yr]	2,57E-09	2,10E-09	1,39E-10	2,94E-10	3,57E-11

ReCiPe 2016 v1.1 Endpoint (E) - Climate change Terrest Ecosystems, default, excl biogenic carbon [species.yr]	9,43E-05	7,71E-05	5,09E-06	1,08E-05	1,31E-06
ReCiPe 2016 v1.1 Endpoint (E) - Freshwater Consumption, Freshw Ecosystems [species.yr]	2,86E-11	1,79E-11	2,58E-12	7,45E-12	6,02E-13
ReCiPe 2016 v1.1 Endpoint (E) - Freshwater Consumption, Terrest Ecosystems [species.yr]	2,22E-07	1,39E-07	2,00E-08	5,78E-08	4,67E-09
ReCiPe 2016 v1.1 Endpoint (E) - Freshwater ecotoxicity [species.yr]	1,22E-04	1,07E-04	6,27E-06	8,02E-06	1,01E-06
ReCiPe 2016 v1.1 Endpoint (E) - Freshwater Eutrophication [species.yr]	6,27E-07	4,39E-07	6,81E-08	1,08E-07	1,22E-08
ReCiPe 2016 v1.1 Endpoint (E) - Land use [species.yr]	1,31E-05	1,29E-05	3,27E-08	1,38E-07	1,25E-08
ReCiPe 2016 v1.1 Endpoint (E) - Marine ecotoxicity [species.yr]	3,35E-05	2,10E-05	2,42E-06	9,80E-06	2,65E-07
ReCiPe 2016 v1.1 Endpoint (E) - Marine Eutrophication [species.yr]	1,55E-10	1,06E-10	1,76E-11	2,84E-11	3,21E-12
ReCiPe 2016 v1.1 Endpoint (E) - Photochemical Ozone Formation, Ecosystems [species.yr]	1,81E-06	1,55E-06	8,10E-08	1,63E-07	2,09E-08
ReCiPe 2016 v1.1 Endpoint (E) - Terrestrial Acidification [species.yr]	3,10E-06	2,53E-06	1,27E-07	3,75E-07	7,59E-08
ReCiPe 2016 v1.1 Endpoint (E) - Terrestrial ecotoxicity [species.yr]	9,07E-04	7,94E-04	4,65E-05	5,96E-05	7,52E-06
ReCiPe 2016 v1.1 Endpoint (E) - Fossil depletion [\$]	156,00	140,00	4,03	10,30	1,47
ReCiPe 2016 v1.1 Endpoint (E) - Metal depletion [\$]	128,00	122,00	1,03	5,00	0,07
ReCiPe 2016 v1.1 (E/A), excl biogenic carbon (Impact / kWh_{th})	284	262	5,12	15,5	1,54

Table 14. Complete impact categories data: Thermocline TES and HTF System, First scenario.

Impact categories in ReCiPe 2016 v1.1 (E/A)	Thermocline configuration: First scenario					
	Total	Molten salts	Reinforcing steel	Chromium steel 18/8	Stone wool	Steel slag pebbles
ReCiPe 2016 v1.1 Endpoint (E) - Climate change Human Health, default, excl biogenic carbon [DALY]	4,30E-02	1,54E-02	1,61E-03	3,40E-03	4,14E-04	2,22E-02
ReCiPe 2016 v1.1 Endpoint (E) - Fine Particulate Matter Formation [DALY]	5,14E-03	2,13E-03	1,58E-04	6,59E-04	5,55E-05	2,13E-03
ReCiPe 2016 v1.1 Endpoint (E) - Freshwater Consumption, Human Health [DALY]	3,87E-05	9,16E-06	2,08E-06	6,01E-06	4,86E-07	2,10E-05
ReCiPe 2016 v1.1 Endpoint (E) - Human toxicity, cancer [DALY]	3,99E-01	1,17E-02	2,89E-02	1,14E-01	3,92E-04	2,44E-01
ReCiPe 2016 v1.1 Endpoint (E) - Human toxicity, non-cancer [DALY]	1,09E-01	2,71E-02	5,21E-03	1,37E-02	1,45E-03	6,18E-02

ReCiPe 2016 v1.1 Endpoint (E) - Ionizing Radiation [DALY]	1,24E-06	2,73E-07	6,88E-08	3,32E-07	2,02E-08	5,47E-07
ReCiPe 2016 v1.1 Endpoint (E) - Photochemical Ozone Formation, Human Health [DALY]	9,73E-06	4,20E-06	3,33E-07	6,98E-07	8,52E-08	4,41E-06
ReCiPe 2016 v1.1 Endpoint (E) - Stratospheric Ozone Depletion [DALY]	1,55E-06	7,97E-07	4,66E-08	1,58E-07	1,02E-08	5,33E-07
ReCiPe 2016 v1.1 Endpoint (E) - Climate change Freshw Ecosystems, default, excl biogenic carbon [species.yr]	2,35E-09	8,42E-10	8,78E-11	1,86E-10	2,26E-11	1,21E-09
ReCiPe 2016 v1.1 Endpoint (E) - Climate change Terrest Ecosystems, default, excl biogenic carbon [species.yr]	8,61E-05	3,09E-05	3,22E-06	6,80E-06	8,28E-07	4,44E-05
ReCiPe 2016 v1.1 Endpoint (E) - Freshwater Consumption, Freshw Ecosystems [species.yr]	3,03E-11	7,18E-12	1,63E-12	4,71E-12	3,81E-13	1,64E-11
ReCiPe 2016 v1.1 Endpoint (E) - Freshwater Consumption, Terrest Ecosystems [species.yr]	2,35E-07	5,57E-08	1,26E-08	3,65E-08	2,96E-09	1,27E-07
ReCiPe 2016 v1.1 Endpoint (E) - Freshwater ecotoxicity [species.yr]	1,06E-04	4,28E-05	3,96E-06	5,07E-06	6,42E-07	5,32E-05
ReCiPe 2016 v1.1 Endpoint (E) - Freshwater Eutrophication [species.yr]	8,99E-07	1,76E-07	4,30E-08	6,84E-08	7,70E-09	6,04E-07
ReCiPe 2016 v1.1 Endpoint (E) - Land use [species.yr]	5,52E-06	5,16E-06	2,07E-08	8,71E-08	7,90E-09	2,44E-07
ReCiPe 2016 v1.1 Endpoint (E) - Marine ecotoxicity [species.yr]	3,34E-05	8,39E-06	1,53E-06	6,20E-06	1,68E-07	1,71E-05
ReCiPe 2016 v1.1 Endpoint (E) - Marine Eutrophication [species.yr]	1,79E-10	4,23E-11	1,11E-11	1,79E-11	2,03E-12	1,05E-10
ReCiPe 2016 v1.1 Endpoint (E) - Photochemical Ozone Formation, Ecosystems [species.yr]	1,47E-06	6,18E-07	5,12E-08	1,03E-07	1,32E-08	6,82E-07
ReCiPe 2016 v1.1 Endpoint (E) - Terrestrial Acidification [species.yr]	2,41E-06	1,01E-06	8,01E-08	2,37E-07	4,80E-08	1,03E-06
ReCiPe 2016 v1.1 Endpoint (E) - Terrestrial ecotoxicity [species.yr]	7,84E-04	3,17E-04	2,94E-05	3,77E-05	4,76E-06	3,95E-04
ReCiPe 2016 v1.1 Endpoint (E) - Fossil depletion [\$]	93,80	56,00	2,55	6,51	0,93	27,73
ReCiPe 2016 v1.1 Endpoint (E) - Metal depletion [\$]	61,10	48,70	0,65	3,16	0,05	8,47
ReCiPe 2016 v1.1 (E/A), excl biogenic carbon (Impact / kWh_{th})	155	105	3,24	9,81	0,98	36,53

Table 15. Complete impact categories data: Thermocline TES and HTF System, Second scenario.

Impact categories in ReCiPe 2016 v1.1 (E/A)	Thermocline configuration: Second scenario					
	Total	Molten salts	Reinforcing steel	Chromium steel 18/8	Stone wool	Steel slag pebbles
ReCiPe 2016 v1.1 Endpoint (E) - Climate change Human Health, default, excl biogenic carbon [DALY]	4,17E-02	7,71E-03	1,30E-03	2,74E-03	3,34E-04	2,96E-02
ReCiPe 2016 v1.1 Endpoint (E) - Fine Particulate Matter Formation [DALY]	4,61E-03	1,07E-03	1,28E-04	5,32E-04	4,48E-05	2,84E-03
ReCiPe 2016 v1.1 Endpoint (E) - Freshwater Consumption, Human Health [DALY]	3,94E-05	4,58E-06	1,68E-06	4,85E-06	3,92E-07	2,79E-05
ReCiPe 2016 v1.1 Endpoint (E) - Human toxicity, cancer [DALY]	4,46E-01	5,86E-03	2,33E-02	9,17E-02	3,16E-04	3,25E-01
ReCiPe 2016 v1.1 Endpoint (E) - Human toxicity, non-cancer [DALY]	1,12E-01	1,36E-02	4,21E-03	1,10E-02	1,17E-03	8,24E-02
ReCiPe 2016 v1.1 Endpoint (E) - Ionizing Radiation [DALY]	1,20E-06	1,36E-07	5,55E-08	2,68E-07	1,63E-08	7,29E-07
ReCiPe 2016 v1.1 Endpoint (E) - Photochemical Ozone Formation, Human Health [DALY]	8,89E-06	2,10E-06	2,69E-07	5,63E-07	6,87E-08	5,89E-06
ReCiPe 2016 v1.1 Endpoint (E) - Stratospheric Ozone Depletion [DALY]	1,28E-06	3,99E-07	3,76E-08	1,27E-07	8,25E-09	7,11E-07
ReCiPe 2016 v1.1 Endpoint (E) - Climate change Freshw Ecosystems, default, excl biogenic carbon [species.yr]	2,27E-09	4,21E-10	7,09E-11	1,50E-10	1,82E-11	1,61E-09
ReCiPe 2016 v1.1 Endpoint (E) - Climate change Terrest Ecosystems, default, excl biogenic carbon [species.yr]	8,34E-05	1,54E-05	2,60E-06	5,49E-06	6,68E-07	5,91E-05
ReCiPe 2016 v1.1 Endpoint (E) - Freshwater Consumption, Freshw Ecosystems [species.yr]	3,09E-11	3,59E-12	1,31E-12	3,80E-12	3,07E-13	2,19E-11
ReCiPe 2016 v1.1 Endpoint (E) - Freshwater Consumption, Terrest Ecosystems [species.yr]	2,40E-07	2,78E-08	1,02E-08	2,95E-08	2,39E-09	1,70E-07
ReCiPe 2016 v1.1 Endpoint (E) - Freshwater ecotoxicity [species.yr]	1,00E-04	2,14E-05	3,20E-06	4,09E-06	5,18E-07	7,10E-05
ReCiPe 2016 v1.1 Endpoint (E) - Freshwater Eutrophication [species.yr]	9,89E-07	8,78E-08	3,47E-08	5,51E-08	6,21E-09	8,05E-07
ReCiPe 2016 v1.1 Endpoint (E) - Land use [species.yr]	3,00E-06	2,58E-06	1,67E-08	7,02E-08	6,37E-09	3,25E-07
ReCiPe 2016 v1.1 Endpoint (E) - Marine ecotoxicity [species.yr]	3,33E-05	4,20E-06	1,24E-06	5,00E-06	1,35E-07	2,27E-05
ReCiPe 2016 v1.1 Endpoint (E) - Marine Eutrophication [species.yr]	1,87E-10	2,11E-11	8,98E-12	1,45E-11	1,64E-12	1,40E-10
ReCiPe 2016 v1.1 Endpoint (E) - Photochemical Ozone Formation, Ecosystems [species.yr]	1,35E-06	3,09E-07	4,13E-08	8,33E-08	1,07E-08	9,09E-07
ReCiPe 2016 v1.1 Endpoint (E) - Terrestrial Acidification [species.yr]	2,18E-06	5,05E-07	6,46E-08	1,91E-07	3,87E-08	1,38E-06
ReCiPe 2016 v1.1 Endpoint (E) - Terrestrial ecotoxicity [species.yr]	7,43E-04	1,59E-04	2,37E-05	3,04E-05	3,84E-06	5,26E-04
ReCiPe 2016 v1.1 Endpoint (E) - Fossil depletion [\$]	73,10	28,00	2,06	5,25	0,75	37,04

ReCiPe 2016 v1.1 Endpoint (E) - Metal depletion [\$]	38,80	24,40	0,53	2,55	0,04	11,30
ReCiPe 2016 v1.1 (E/A), excl biogenic carbon (Impact / kWh_{th})	112	52	2,61	7,91	0,79	48,74

Tabla 16. Complete impact categories data: Global environmental impacts associated to the CSP plant

Impact categories in ReCiPe 2016 v1.1 (E/A)	Conventional configuration		Thermocline: First scenario		Thermocline: Second scenario	
	Total	Relative (%)	Total	Relative (%)	Total	Relative (%)
ReCiPe 2016 v1.1 Endpoint (E) - Climate change Human Health, default, excl biogenic carbon [DALY]	4,71E-05	3,03E-02	4,61E-05	3,67E-02	4,58E-05	3,96E-02
ReCiPe 2016 v1.1 Endpoint (E) - Fine Particulate Matter Formation [DALY]	6,33E-06	4,08E-03	5,97E-06	4,75E-03	5,85E-06	5,05E-03
ReCiPe 2016 v1.1 Endpoint (E) - Freshwater Consumption, Human Health [DALY]	1,49E-07	9,58E-05	1,49E-07	1,19E-04	1,49E-07	1,29E-04
ReCiPe 2016 v1.1 Endpoint (E) - Human toxicity, cancer [DALY]	4,50E-04	0,29	0,000483	0,39	4,94E-04	0,427
ReCiPe 2016 v1.1 Endpoint (E) - Human toxicity, non-cancer [DALY]	6,31E-04	0,407	0,000633	0,5	6,34E-04	0,547
ReCiPe 2016 v1.1 Endpoint (E) - Ionizing Radiation [DALY]	2,07E-09	1,33E-06	2,05E-09	1,63E-06	2,04E-09	1,76E-06
ReCiPe 2016 v1.1 Endpoint (E) - Photochemical Ozone Formation, Human Health [DALY]	1,16E-08	7,47E-06	1,10E-08	8,77E-06	1,08E-08	9,35E-06
ReCiPe 2016 v1.1 Endpoint (E) - Stratospheric Ozone Depletion [DALY]	1,86E-09	1,20E-06	1,68E-09	1,34E-06	1,62E-09	1,40E-06
ReCiPe 2016 v1.1 Endpoint (E) - Climate change Freshw Ecosystems, default, excl biogenic carbon [species.yr]	2,57E-12	1,65E-09	2,52E-12	2,00E-09	2,50E-12	2,16E-09
ReCiPe 2016 v1.1 Endpoint (E) - Climate change Terrest Ecosystems, default, excl biogenic carbon [species.yr]	9,41E-08	6,07E-05	9,22E-08	7,34E-05	9,16E-08	7,91E-05
ReCiPe 2016 v1.1 Endpoint (E) - Freshwater Consumption, Freshw Ecosystems [species.yr]	1,17E-13	7,51E-11	1,17E-13	9,31E-11	1,17E-13	1,01E-10
ReCiPe 2016 v1.1 Endpoint (E) - Freshwater Consumption, Terrest Ecosystems [species.yr]	9,04E-10	5,83E-07	9,07E-10	7,22E-07	9,08E-10	7,85E-07
ReCiPe 2016 v1.1 Endpoint (E) - Freshwater ecotoxicity [species.yr]	1,22E-07	7,87E-05	1,18E-07	9,42E-05	1,17E-07	1,01E-04
ReCiPe 2016 v1.1 Endpoint (E) - Freshwater Eutrophication [species.yr]	1,41E-09	9,07E-07	1,47E-09	1,17E-06	1,49E-09	1,29E-06
ReCiPe 2016 v1.1 Endpoint (E) - Land use [species.yr]	3,93E-09	2,54E-06	2,20E-09	1,75E-06	1,62E-09	1,40E-06
ReCiPe 2016 v1.1 Endpoint (E) - Marine ecotoxicity [species.yr]	6,96E-08	4,48E-05	6,95E-08	5,53E-05	6,95E-08	6,00E-05
ReCiPe 2016 v1.1 Endpoint (E) - Marine Eutrophication [species.yr]	2,22E-13	1,43E-10	2,28E-13	1,81E-10	2,29E-13	1,98E-10

ReCiPe 2016 v1.1 Endpoint (E) - Photochemical Ozone Formation, Ecosystems [species.yr]	1,73E-09	1,11E-06	1,65E-09	1,31E-06	1,62E-09	1,40E-06
ReCiPe 2016 v1.1 Endpoint (E) - Terrestrial Acidification [species.yr]	4,23E-09	2,73E-06	4,07E-09	3,24E-06	4,02E-09	3,47E-06
ReCiPe 2016 v1.1 Endpoint (E) - Terrestrial ecotoxicity [species.yr]	9,04E-07	5,83E-04	8,76E-07	6,97E-04	8,66E-07	7,48E-04
ReCiPe 2016 v1.1 Endpoint (E) - Fossil depletion [\$]	0,108	69,5	0,0936	74,6	0,089	76,8
ReCiPe 2016 v1.1 Endpoint (E) - Metal depletion [\$]	0,046	29,7	0,0308	24,5	0,026	22,2
ReCiPe 2016 v1.1 (E/E), excl biogenic carbon (Impact / kWh)	0,155	100	0,126	100	0,116	100

Abstract

There is a demand for alternative thermal energy storage (TES) materials to support the global deployment of concentrated solar power (CSP) plants. These materials should fulfil specific criteria concerning technical, economic, and ecological performance.

This research work focuses on the comparative life cycle assessment (LCA) of a concentrating solar power (CSP) plant that utilizes Electric Arc Furnace (EAF) steel slag as a thermal energy storage material in a thermocline configuration, compared to a conventional CSP plant that uses molten salts. The study aims to evaluate the potential environmental impacts and identify opportunities for sustainability improvement in CSP plants technology.

The results demonstrate a significant reduction in the material inventory demand and in the overall environmental impact for the scenarios where the thermocline configuration was chosen. The thermocline TES system showcases notable reductions in the following environmental impact indicators: a) "Damage to the resources availability" and b) "Global warming potential".

Thus, the study highlights the potential of using steel slag to improve the sustainability of CSP plants, while revalorising materials that otherwise could finish in a landfill. The research and analysis performed indicate that the use of steel slag as a thermal storage material is technically feasible and it has the potential to increase the environmental and economic sustainability, as this material is abundant, energy efficient and sustainable enough for industrial scale applications. In fact, the use of steel slag as TES material could contribute positively to the Sustainable Development Goals (SDGs) through: including cleaner energy solutions, promoting innovation in green power generation, responsible managing of resources, and mitigating the climate change.

Resumen

Existe una demanda de materiales provenientes de sistemas alternativos para el almacenamiento de energía térmica que permitan impulsar el despliegue mundial de plantas de concentración de energía solar. Estos materiales deben cumplir criterios específicos de rendimiento técnico, económico y ecológico.

Este trabajo de investigación se centra en la evaluación comparativa del análisis del ciclo de vida de una planta de concentración de energía solar que utiliza escoria de acero de horno de arco eléctrico como material de almacenamiento térmico (en una configuración de termoclina), respecto a una planta convencional de concentración de energía solar que utiliza sal solar. El estudio evalúa los potenciales impactos ambientales e identifica oportunidades de mejora de la sostenibilidad para estas centrales de generación eléctrica.

Los resultados demuestran una reducción significativa de la demanda de materiales y del impacto medioambiental en los escenarios donde se considera una configuración de termoclina. El sistema de almacenamiento térmico en termoclina muestra notables reducciones en los siguientes indicadores de impacto ambiental: a) "Daño a la disponibilidad de recursos" y b) "Potencial de calentamiento global".

Así, este estudio pone de manifiesto el potencial que tiene utilizar la escoria de acero para mejorar la sostenibilidad de las plantas de concentración de energía solar, ya que se revaloriza un material que, en otro caso, podría acabar en un vertedero. La investigación y el análisis realizados indican que el uso de escoria de acero es técnicamente viable, y que este tiene el potencial para incrementar la sostenibilidad medioambiental y económica de estas plantas, ya que este material es abundante, energéticamente eficiente y lo suficientemente sostenible para aplicaciones a escala industrial. De hecho, el uso de escoria de acero como material de almacenamiento térmico puede contribuir positivamente a los Objetivos de Desarrollo Sostenible (ODS) a través de: la inclusión de soluciones energéticas más limpias, la promoción de la innovación en la generación de energía verde, la gestión responsable de los recursos, y la mitigación del cambio climático.